

A Bregman-Sinkhorn Algorithm for the Maximum Weight Independent Set Problem

Stefan Haller*, Bogdan Savchynskyy

Heidelberg University

Abstract

We propose a scalable approximate algorithm for the NP-hard maximum-weight independent set problem. The core component of our algorithm is a dual coordinate descent applied to a smoothed LP relaxation of the problem. This technique is commonly known by the names *Bregman method* and *Sinkhorn algorithm* in the literature. Our algorithm addresses a family of *clique cover LP relaxations*, where the constraints are determined by the set of cliques covering the underlying graph. The objective function of the relaxation is smoothed with an entropy term. A crucial aspect determining efficiency of our approach is controlling the smoothing level during the optimization process. While several dedicated techniques have been considered in the literature to this end, we propose a new one based on estimation of the relaxed duality gap. To make this estimation possible, we developed a new projection method to the feasible set of the considered LP relaxation. We experimentally show that our smoothing scheduling significantly outperforms the standard one based on feasibility estimation. Additionally to solving the relaxed dual, we utilize a simple and very efficient primal heuristic to obtain feasible integer solutions of the original non-relaxed problem. Our heuristic is a combination of randomized greedy generation and optimal recombination applied to the reduced costs computed by the dual optimization. Our experimental validation considers two datasets rooted in real-world applications, where our method demonstrates the ability to discover high-quality approximate solutions within 10 seconds for graphs with up to 882 thousand nodes and 344 million edges.

1 Introduction

Let $\mathcal{G} = (\mathcal{V}, \mathcal{E})$ be a undirected graph with a *node set* \mathcal{V} and an *edge set* $\mathcal{E} \subseteq \binom{\mathcal{V}}{2}$. An *independent* or *stable set* is the subset of mutually non-adjacent vertices $\mathcal{V}' \subseteq \mathcal{V}$,

e.g., for any $i, j \in \mathcal{V}'$ it holds $\{i, j\} \notin \mathcal{E}$. Given the costs $c_i, i \in \mathcal{V}$, the *maximum weight independent set* (MWIS) problem consists in finding an independent set with the maximum total cost.

The problem has applications in computer vision [5], [28, Ch.7], vehicle routing [9], transmission scheduling in wireless networks [33] and is one of the classical combinatorial optimization problems [12]. It is NP-hard, since its unweighted variant is NP-complete [20].¹ Therefore, various relaxations and approximation algorithms addressing this problem have been proposed.

We consider a family of *clique cover relaxations* for this problem and propose a scalable dual algorithm. We build upon it with an efficient primal heuristic that profits from the reduced costs computed by the dual algorithm. In total, this leads to an efficient and well-scalable MWIS method.

Notation. Vectors are **bold** and scalars not: \mathbf{x} is a vector and x is a scalar. Scalar operations and relations are applied to vectors component-wise: $\mathbf{x} \geq \mathbf{0}$ means non-negativity of all coordinates of \mathbf{x} and $\log \mathbf{x}$ is a vector of coordinate logarithms. $\mathbb{R}_{\geq 0}^n := \{x \in \mathbb{R}^n \mid x \geq 0\}$, $[n] := \{1, 2, \dots, n\}$. $\llbracket A \rrbracket$ are Iverson brackets equal to 1 if A holds, otherwise 0. *Overview of the notation that will be introduced later in the paper:*

- \mathbf{x} – primal variables
- \mathbf{c} – cost vector (Section 1)
- $\boldsymbol{\lambda}$ – dual variables
- \mathbf{c}^λ – vector of reduced costs (Section 4)
- $\bar{K}_j = K_j \cup \{x_{n+j}\}, j \in [m]$ – cliques with and without slack variables x_{n+j} (Section 1);
- $J_i = \{j \in [m] \mid \bar{K}_j \ni i\}$ – set of cliques containing variable x_i (Section 4);
- $C = \{x \in [0, 1]^{n+m} \mid \sum_{i \in \bar{K}_j} x_i = 1, j \in [m]\}$ – feasible set of the relaxed problem (3) (Section 7.3).

* This research was partially conducted during the author's employment at rabbitAI GmbH.

¹ The *vertex cover problem* reducible to the maximum independent set problem is considered.

2 Overview of the known results and related work

The MWIS problem is also known as *maximum weight stable set* or *vertex packing* and is mutually reducible to the *minimum weight vertex cover*, *maximum weight clique* and *weighted set packing* problems [17, 10]. Algorithms addressing these problems can be *straightforwardly* applied to MWIS and vice versa. Many theoretical results are shared by these problems as well. Yet, we will stick to the MWIS problem formulation in the following.

ILP formulation and edge relaxation. Let $[n]$ denote $\{1, 2, \dots, n\}$ and assume that the set of graph nodes consists of n elements, i.e., $\mathcal{V} = [n]$. We introduce a binary variable $x_i \in \{0, 1\}$ for each node $i \in \mathcal{V}$. If $x_i = 1$, it indicates that node i is part of the maximum-weight independent set. This results in a natural integer linear program (ILP) formulation of the MWIS problem:

$$\begin{aligned} \max_{\mathbf{x} \in \{0,1\}^n} \quad & \langle \mathbf{c}, \mathbf{x} \rangle \\ \text{s.t.} \quad & x_i + x_j \leq 1, \{i, j\} \in \mathcal{E}. \end{aligned} \quad (1)$$

The respective LP relaxation, obtained by substituting the integer constraints $\mathbf{x} \in \{0, 1\}^n$ with the box constraints $\mathbf{x} \in [0, 1]^n$, is referred to as the *edge relaxation*. The edge relaxation is well-known to be tight for bipartite graphs [24] and can be reduced to minimum s-t cut problems (or to equivalent maximum flows), allowing it to be efficiently solved [24, 17]. The efficient solvability of the edge relaxation follows from its two interrelated properties [24]: First, its corresponding polytope has only *half-integral* vertices, meaning that all basic solutions of the relaxation have coordinates in the set $\{0, 1/2, 1\}$. Second, it exhibits the *persistence* property: All coordinates of a relaxed solution with integer values (0 or 1) belong to some (but the same) optimal solution of the non-relaxed problem (1). This persistence property has been particularly useful in improving approximation bounds for several primal heuristics, as demonstrated in works such as [17, 18].

However, the edge relaxation has its limitations: It gets loose for dense graphs, as demonstrated by the following statement:

Proposition 1. *Let G be fully-connected, all costs positive, $c_j > 0$, $j \in \mathcal{V}$, and $c_i < \sum_{j \in \mathcal{V} \setminus \{i\}} c_j$ for $i = \arg \max_{j \in \mathcal{V}} c_j$. Then the edge relaxation has a unique solution $(\underbrace{1/2, 1/2, \dots, 1/2}_n)$.*

Note that costs positivity can be assumed w.l.o.g. for the MWIS problem. Nodes with non-positive costs can be excluded from the graph together with their incident edges without influencing the optimal objective value.

Proposition 1, proved in Section 13, shows that the edge relaxation may not reveal *any* information about optimal solutions of the non-relaxed problem (1) for dense

graphs. To address this limitation, the *clique constraints* and the respective *clique relaxation* are considered for the MWIS problem in the literature [31], [37, Sec. 64]. Before defining it, we first introduce a family of relaxations that includes both the edge and the clique relaxations.

Clique cover relaxation family. Let $K_j \subseteq \mathcal{V}$, $j \in [m]$, be subsets of nodes such, that the respective induced subgraphs of G are cliques. Abusing notation, we will refer to K_j themselves as *cliques*. We assume that K_j , $j \in [m]$, cover all edges and nodes of the graph, e.g. $\mathcal{E} = \bigcup_{j=1}^m \{\{i, i'\} \mid i, i' \in K_j\}$, $\mathcal{V} = \bigcup_{j=1}^m \{i \mid i \in K_j\}$, and, therefore, are referred to as a *clique cover*.² We define the *clique cover ILP formulation* of the MWIS problem as

$$\begin{aligned} \max_{\mathbf{x} \in \{0,1\}^n} \quad & \langle \mathbf{c}, \mathbf{x} \rangle \\ \text{s.t.} \quad & \sum_{i \in K_j} x_i \leq 1, j \in [m]. \end{aligned} \quad (2)$$

Its natural LP relaxation, further referred to as *clique cover relaxation* is obtained by substituting integer constraints $\mathbf{x} \in \{0, 1\}^n$ with the respective box constraints $\mathbf{x} \in [0, 1]^n$. The relaxation of (2) is called *clique relaxation*, if the set $\{K_j \mid j \in [m]\}$, consists of *all* cliques of G .

Whereas the solutions of the non-relaxed problems (1) and (2) coincide, their relaxations may differ significantly. In particular, the clique relaxation lacks both the half-integrality and persistency properties in general [31]. Furthermore, it does not admit a reduction to any efficiently solvable LP subclass like the min-cost-flow problem. This is because its relaxation is as difficult as linear programs in general [29]. However, it has the advantage of being a tighter relaxation in general, as shown by the following statement:

Proposition 2. *Let K_j , $j \in [m]$, and K'_j , $j \in [m']$, be two clique covers of the graph G such that for every K'_j , $j \in [m']$, there is $l \in [m]$: $K'_j \subseteq K_l$. Then the relaxation determined by K_j , $j \in [m]$, is at least as tight as the relaxation determined by K'_j , $j \in [m']$.*

Proposition 2 defines a partial order on the set of clique cover relaxations with respect to their tightness. The edge relaxation is the least tight and constitutes the minimum with respect to this partial order. The maximum is determined by the clique relaxation. According to Proposition 2, the latter is equivalent to the relaxation, where K_j , $j \in [m]$, consists of maximal cliques (i.e., those that are not subgraphs of any other clique) only. It is also known that clique inequalities are facet-defining for the stable set polytope³ if and only if the respective clique is maximal [37].

Considering the same setting as in Proposition 1, one obtains the following result:

² The covering of nodes in addition to the covering of edges is required to deal with isolated nodes.

³ The convex hull of all feasible solutions of (1).

Proposition 3. *The maximal clique relaxation, defined by the single maximal clique, is tight for complete graphs.*

Unfortunately, the number of maximal cliques may grow exponentially with the graph size in general [23]. Hence, in practice, one has to ideally consider a clique cover consisting of a subset of the maximal cliques, although the algorithms we describe in this paper are applicable to arbitrary clique covers.

Equality formulation. Note that the clique constraints in (2) can be turned to equality by introducing m slack variables x_{n+j} , $j \in [m]$, and assuming $c_{n+j} = 0$ and $\bar{K}_j = K_j \cup \{n+j\}$. The respective LP relaxation takes the form:⁴

$$\begin{aligned} \max_{\mathbf{x} \in [0,1]^{n+m}} \quad & \langle \mathbf{c}, \mathbf{x} \rangle \\ \text{s.t.} \quad & \sum_{i \in \bar{K}_j} x_i = 1, j \in [m]. \end{aligned} \quad (3)$$

As (3) is equivalent to the clique cover relaxation, we will primarily use this name to refer to (3) unless otherwise stated. Likewise, the non-trivial constraints of (3) will be called *clique constraints* just like those in (2). To avoid ambiguity we will reference the specific formula.

Remark 1. *The box constraints $\mathbf{x} \in [0,1]^{n+m}$ in (3) can be substituted with the non-negativity constraints $\mathbf{x} \geq \mathbf{0}$ without changing the feasible set of the problem. This is because $\mathbf{x} \leq \mathbf{1}$ due to the clique constraints in (3), as cliques cover all vertices of the underlying graph. In the following we stick to the box constraints for technical reasons.*

Relation to pseudo-boolean optimization. There is a natural equivalence between MWIS and pseudo-boolean optimization [3]. More precisely, the MWIS problem (1) with non-negative costs c can be reduced to, e.g., maximization over $\mathbf{x} \in \{0,1\}^n$ of the following *posiform* [3, Thm.4]:

$$\phi(x_1, \dots, x_n) = \sum_{i \in [n]} c_i x_i \cdot \prod_{j: \{i,j\} \in \mathcal{E}} \bar{x}_j. \quad (4)$$

The term *posiform* comes from the non-negativity of the coefficients c_i .

In the other direction, maximization of an arbitrary posiform $f(x_1, \dots, x_n) = \sum_{i=1}^p c_i T_i + c_0$, where $c_i \geq 0$, $i \in \{0, \dots, p\}$, and $T_i = \prod_{j \in A_i} x_j \prod_{k \in B_i} \bar{x}_k$ with $A_i, B_i \subseteq [n]$ and $A_i \cap B_i = \emptyset$, is reducible to MWIS defined over the so called *conflict graph* [3, Thm. 3].

It is known that any pseudo-boolean function can be represented as a posiform up to a constant [3, Prop. 1]. Also, setting all negative costs in (1) to zero preserves the

optimal value and may only enlarge the set of optimal solutions. This implies equivalence of MWIS and pseudo-boolean optimization and allows for cross-application of optimization techniques from both domains.

A special case of this relation is a reduction of MWIS (1) by considering a sufficiently large $M > 0^5$ to the maximization of the *quadratic* pseudo-boolean function

$$\sum_{i=1}^n c_i x_i - M \cdot \sum_{\{i,j\} \in \mathcal{E}} x_i x_j. \quad (5)$$

The latter, in turn, has a one-to-one correspondence to the *binary pairwise discrete energy minimization problem* [34, Ch. 12]. The respective *local polytope* relaxation [34, Ch. 4] is equivalent to the edge relaxation [33]. Some MWIS algorithms therefore adopt techniques from the field of discrete graphical models [33, 38], however, their guaranteed performance does not go beyond the edge relaxation.

We use the transformation (5) in Section 9 for a primal heuristic supplementing our dual method.

Solvability and approximation. The MWIS problem is polynomially solvable for perfect graphs [14]. In particular, this applies to bipartite graphs mentioned above. Efficient methods also exist for other graph families, see [37, Ch. 64.9a] for an overview. Contrary to the closely related vertex cover problem, there are no constant factor approximation algorithms for MWIS [41]. A number of approximation bounds has been obtained for the general problem as well as for its special cases [17, 26], especially wrt. to the maximum degree of the underlying graph [18]. These algorithms often make use of the persistency property of the edge relaxation.

Primal heuristics is a popular class of algorithms addressing MWIS, see e.g., [5, 7, 25, 30] and references therein. Apart from the direct application, they can be used in combination with the relaxation-based methods, as in [7] and this work, or, e.g., within reduction-based methods [22]. We get back to the first case in Section 9 and empirically compare to algorithms of both types in Section 10.

Relation to linear assignment. The MWIS problem (2) can be seen as a generalization of the *incomplete* linear assignment problem [6], as the ILP formulation of the latter, namely

$$\begin{aligned} \max_{\mathbf{x} \in \{0,1\}^{n \times m}} \quad & \langle \mathbf{c}, \mathbf{x} \rangle \\ \text{s.t.} \quad & \sum_{i \in [n]} x_{ij} \leq 1, j \in [m], \\ & \sum_{j \in [m]} x_{ij} \leq 1, i \in [n], \end{aligned} \quad (6)$$

⁴ The respective ILP formulation is a special case of the *weighted set partitioning* problem.

⁵ It is sufficient to consider $M > \max_{i \in V} c_i$.

is a special case of (2). Incomplete linear assignment is tightly related and reducible to the (complete) linear assignment problem [6, 16] in linear time. From the other viewpoint, linear assignment is a specialization of the optimal transport problem. These facts are important, as the Sinkhorn algorithm and its variants [27] have shown their remarkable efficiency and scalability for the optimal transport problems. The Sinkhorn algorithm itself [39] is a special case of the famous Bregman method for linear programs [4], which is one of the widely considered entropy optimization techniques [11]. This leads us to the main contribution of our work formulated below.

3 Contribution and paper content

We propose a scalable iterative algorithm for the clique cover family of relaxations (3). The algorithm is based on the Bregman method and, therefore, is essentially a smoothed dual coordinate minimization. Our method can be also seen as a generalization of the Sinkhorn algorithm for optimal transport. We propose several variations of our method, with different numerics, scheduling of the smoothing level and sparsity-based speed-up. As a dual method, it operates over the feasible set of the dual problem, but the respective relaxed primal variables remain infeasible upon convergence. We propose an efficient method to *project* them to the feasible set of the primal relaxed problem. This leads to feasible primal estimates of the relaxed solution and, as a result, to estimates of the duality gap. In turn, the duality gap estimate results in a new smoothing scheduling method that consistently outperforms the standard feasibility-based scheduling in our experiments.

Convergence of our algorithms follows from those of the Bregman method. Empirically, it is able to attain high quality approximations of the relaxed problem. On large-scale instances (with more than 100 000 graph edges) it is notably faster than simplex or interior point methods.

We combine the dual algorithm with a simple but efficient primal heuristic to address the non-relaxed MWIS problem. In our experimental evaluation we were able to find good approximate solutions for large-scale problem instances significantly faster than off-the-shelf Gurobi ILP solver [15] as well as the reduction-based methods [22]. Our method outperforms also the recently published meta-heuristic [7, 8] in terms of speed as well as the attained objective values.

Our code is publicly available on GitHub⁶.

Paper content. We analyze the clique cover relaxation (3) and its Lagrange dual in Section 4. We start with a simple coordinate minimization method addressing this problem. Although being a natural baseline, it

does not guarantee convergence to the dual optimum as we show.

We introduce the Bregman method and its specialization to the MWIS problem in Section 5. In essence, this method can be seen as a smoothed variant of the above mentioned coordinate minimization algorithm. The amount of smoothing is controlled by a *temperature* parameter. With more smoothing, i.e. high temperature, the algorithm converges faster but the approximation of the original problem gets worse.

Section 6 describes two numerically stable implementations of the introduced Bregman method specialization. These are essentially the same as used with this type of algorithms for optimal transport problems.

Section 7 considers two strategies of smoothing scheduling. Additionally, a projection method to the feasible set that allows us to obtain feasible primal estimates for the relaxed problem is described here.

Section 8 proposes two sparsity-based strategies to speed-up our dual algorithms. Whereas the first strategy is a heuristic, the second is based on upper-bounding of the possible perturbation of the smoothed dual objective value.

In Section 9, we describe a simple primal heuristic to reconstruct integer solutions of the non-relaxed MWIS problem. Though by itself, it is inferior to other similar methods, in combination with our dual algorithm it shows competitive results.

Finally, Section 10 is devoted to the experimental evaluation. Here we consider two benchmarks, related to image segmentation [28] and vehicle routing [9] respectively. Additionally to the experimental study of different variants of our method, we compare it to the Gurobi general purpose LP and ILP solvers and state-of-the-art reduction-based algorithms and primal heuristics [22, 19, 7, 25].

4 Dual of the clique cover relaxation

Dual problem. First, we introduce the constraint sets $J_i = \{j \in [m] \mid \bar{K}_j \ni i\}$ as the set of cliques containing the variable x_i . In particular, for any slack variable x_{n+j} it holds $J_{n+j} = \{j\}$.

By dualizing the equality constraints of the clique cover relaxation (3) we obtain its Lagrange dual problem:

$$\begin{aligned} \min_{\lambda \in \mathbb{R}^m} \left[\max_{x \in [0,1]^{n+m}} \langle c, x \rangle - \sum_{j=1}^m \lambda_j \left(\sum_{i \in \bar{K}_j} x_i - 1 \right) \right] \\ = \min_{\lambda \in \mathbb{R}^m} \underbrace{\left[\sum_{j=1}^m \lambda_j + \max_{x \in [0,1]^{n+m}} \langle c^\lambda, x \rangle \right]}_{D(\lambda)} \quad (7) \end{aligned}$$

where λ are dual variables and $c_i^\lambda = c_i - \sum_{j \in J_i} \lambda_j$ are the *reduced* or *reparametrized* costs. From the first term in (7)

⁶<https://github.com/vislearn/libmopt>

it follows that $\langle \mathbf{c}, \mathbf{x} \rangle = \langle \mathbf{c}^\lambda, \mathbf{x} \rangle + \sum_{j=1}^m \lambda_j$ holds for any \mathbf{x} that satisfies the clique constraints in (3). In other words, the costs of all feasible solutions (that includes integral solutions) of the problem (3), are shifted by the constant $\sum_{j=1}^m \lambda_j$ with the transformation $\mathbf{c} \rightarrow \mathbf{c}^\lambda$. In particular, it implies that the set of optimal solutions of these problems is invariant with respect to this transformation. Therefore, the latter is sometimes referred to as *equivalent transformation* in the literature.

The dual objective $D(\lambda)$ is convex piecewise affine as a maximum of a finite number of affine functions, since $\max_{\mathbf{x} \in [0,1]^{n+m}} \langle \mathbf{c}^\lambda, \mathbf{x} \rangle = \max_{\mathbf{x} \in \{0,1\}^{n+m}} \langle \mathbf{c}^\lambda, \mathbf{x} \rangle$ in (7). By strong duality the minimum of the dual problem (7) coincides with the maximum of the clique relaxation (3).

We introduce the set $\text{Sign}(\mathbf{c}) := \arg \max_{\mathbf{x} \in [0,1]^{n+m}} \langle \mathbf{c}, \mathbf{x} \rangle$. Hence, $\mathbf{x} \in \text{Sign}(\mathbf{c})$ if

$$x_i = \begin{cases} 0, & \text{if } c_i < 0, \\ 1, & \text{if } c_i > 0, \\ \in [0, 1], & \text{if } c_i = 0. \end{cases} \quad (8)$$

The dual value is therefore equal to $D(\lambda) = \sum_{j=1}^m \lambda_j + \langle \mathbf{c}^\lambda, \mathbf{x}^* \rangle$ for any $\mathbf{x}^* \in \text{Sign}(\mathbf{c}^\lambda)$. Different subgradients of D can be obtained for different values of $\mathbf{x}^* \in \text{Sign}(\mathbf{c}^\lambda)$ as

$$\frac{\partial D}{\partial \lambda_j}[\mathbf{x}^*] = 1 + \frac{\partial \langle \mathbf{c}^\lambda, \mathbf{x}^* \rangle}{\partial \lambda_j} = 1 + \left\langle \frac{\partial \mathbf{c}^\lambda}{\partial \lambda_j}, \mathbf{x}^* \right\rangle = 1 - \sum_{i \in \bar{K}_j} x_i^*. \quad (9)$$

The last term counts the number of non-zero coordinates of \mathbf{x}^* in the clique \bar{K}_j . The considered subgradient coordinate $\frac{\partial D}{\partial \lambda_j}[\mathbf{x}^*]$ is equal to 0 if their sum is equal to 1.

In other words, λ is dual optimal if and only if $\text{Sign}(\mathbf{c}^\lambda)$ contains at least one vector feasible for (3). This vector is a solution of the relaxed primal problem:

Proposition 4. *Let $\mathbf{x}^* \in \text{Sign}(\mathbf{c}^\lambda)$ and $\frac{\partial D}{\partial \lambda_j}[\mathbf{x}^*] = 0$ for all $j \in [m]$. Then \mathbf{x}^* is the solution of the respective clique relaxation (3). If additionally $\mathbf{x}^* \in \{0, 1\}^{n+m}$, then its first n coordinates constitute a solution of the non-relaxed problem (2).*

The dual coordinate minimization Algorithm 1 iteratively considers each clique and changes the value of the respective dual variable. This is done such that the largest reduced cost of the nodes belonging to the clique becomes zero.

Being very simple, this algorithm implements the *coordinate minimization* principle. Indeed, the dual objective D is convex. Therefore, its restriction to the j -th variable λ_j is convex as well. In turn, a necessary and sufficient optimality condition for the restricted convex function is existence of a zero subgradient. In this case, after each inner iteration of Algorithm 1 there should exist $\mathbf{x}^* \in \text{Sign}(\mathbf{c}^\lambda)$ such that $\frac{\partial D}{\partial \lambda_j} = 1 - \sum_{i \in \bar{K}_j} x_i^* = 0$ (see (9)) for

Algorithm 1: Dual coordinate descent algorithm.

```

1 while stopping criterion not fulfilled do
    // loop over cliques:
2   for  $j \in [m]$  do
        // turn the max. cost in the clique to 0:
        // pick the clique-largest reduced cost:
3      $i^* \in \arg \max_{i \in \bar{K}_j} c_i^\lambda$ 
        // ... and make it zero
4      $\lambda_j = \lambda_j + c_{i^*}^\lambda$ 

```

Result: λ

the value of j being an index of the currently processed clique. To obtain such \mathbf{x}^* it is sufficient to set $x_{i^*}^* = 1$ and $x_i^* = 0$ for $i \in \bar{K}_j \setminus \{i^*\}$, where i^* is defined as in Algorithm 1.

Unfortunately, coordinate minimization is not guaranteed to converge to the optimum for convex piece-wise affine functions [2, Ch. 2.7]. This holds in general, as well as for the dual (7) in particular, as shown by the following example:

Example 1. Consider an MWIS problem in format (3) with the following $m = 6$ constraints:

$$x_1 + x_2 + x_6 = 1 \quad (10)$$

$$x_2 + x_3 + x_7 = 1 \quad (11)$$

$$x_3 + x_1 + x_8 = 1 \quad (12)$$

$$x_1 + x_3 + x_4 + x_9 = 1 \quad (13)$$

$$x_4 + x_5 + x_{10} = 1 \quad (14)$$

$$x_5 + x_3 + x_{11} = 1 \quad (15)$$

The coordinates with indices 6 and above correspond to the slack variables and can be found in a single equation only. We also assume $c_i^\lambda = 0$ for $i \in [5]$ and $c_i^\lambda < 0$ for $i > 5$.

Obviously this λ is a fix-point of Algorithm 1. We will show that this point is not optimal. For this, it is sufficient to show that the set $\text{Sign}(\mathbf{c}^\lambda)$ does not contain feasible vectors. Assume it does and $\mathbf{x} \in \text{Sign}(\mathbf{c}^\lambda)$, then $x_i = 0$ for $i > 5$ as $c_i^\lambda < 0$. Assume $x_1 = \gamma \geq 0$. This implies $x_2 = 1 - \gamma$, and $x_3 = \gamma = 1 - \gamma = 0.5$ and hence $x_1 = x_2 = x_3 = 0.5$ from the first three constraints. The next two constraints imply $x_4 = 0$ and $x_5 = 1$. The last equality does not hold as $x_5 + x_3 = 1.5 > 1$, which is a contradiction.

Unfortunately, the fix-points attained by Algorithm 1 in our experiments give only a loose approximation of the dual optimum, although the respective lower bounds are usually much better than those of the edge relaxation, see Figure 1(a) in Section 10. Therefore, Algorithm 1 can only be seen as a weak baseline. However, it is very important due to the fact that the convergent algorithms we consider below are its smoothed modifications.

Algorithm 2: Naive Bregman method for MWIS.

Input: $x_i = \exp(c_i/T)$, $i \in [n + m]$

1 **while** stopping criterion not fulfilled **do**

 // loop over cliques:

2 **for** $j \in [m]$ **do**

 // make the sum of x_i within the clique = 1

3 $s := \sum_{i \in \tilde{K}_j} x_i$

4 $x_i := x_i/s$, $\forall i \in \tilde{K}_j$

Result: \mathbf{x}

5 Bregman method for MWIS

The Bregman method [4] can be used to address linear programs $\{\max_{\mathbf{x} \geq 0} \langle \mathbf{c}, \mathbf{x} \rangle, \text{ s.t. } A\mathbf{x} = \mathbf{b}\}$ through solving their approximations $\{\max_{\mathbf{x} \geq 0} \langle \mathbf{c}, \mathbf{x} \rangle + T\mathcal{H}(\mathbf{x}), \text{ s.t. } A\mathbf{x} = \mathbf{b}\}$ with the function \mathcal{H} being differentiable and strictly concave on $\mathbf{x} \geq 0$.⁷ Parameter $T > 0$ is the *temperature* or *smoothing* parameter that regulates the trade-off between approximation accuracy and convergence speed. The latter problem takes the form of the *smoothed clique cover relaxation* in our case:

$$\begin{aligned} & \max_{\mathbf{x} \in [0,1]^{n+m}} \langle \mathbf{c}, \mathbf{x} \rangle + T\mathcal{H}(\mathbf{x}) \\ & \text{s.t. } \sum_{i \in \tilde{K}_j} x_i = 1, j \in [m], \end{aligned} \quad (16)$$

since the box constraints $\mathbf{x} \in [0,1]^{n+m}$ in (16) are equivalent to $\mathbf{x} \geq 0$ as noted in Remark 1.

In our application, as well as in the optimal transport literature [27], the function \mathcal{H} is defined as $\mathcal{H}(\mathbf{x}) := -\sum_{i=1}^{n+m} (x_i \log x_i - x_i)$, i.e., \mathcal{H} is the entropy shifted by a linear function. The latter is used for the sake of resulting formulas.

On each iteration of the Bregman method the current iterate \mathbf{x} is projected to the hyperplane determined by a single row of the constraint matrix A . In case of the function \mathcal{H} defined as above and constraints of the form $\sum_{i \in \tilde{K}_j} x_i = 1$ as in (16), this projection results in *normalization* of the respective coordinates of \mathbf{x} , as given by Algorithm 2. The only computation that depends on the cost vector \mathbf{c} is the initialization of the algorithm: Whereas it converges to a feasible point for *arbitrary* initialization $\mathbf{x} > \mathbf{0}$, its limit point is a solution to the problem (16) only if properly initialized. When applied to the linear assignment problem Algorithm 2 is usually referred to as *Sinkhorn algorithm* due to the seminal paper [39] showing that iterative normalization of a square matrix turns it into a bi-stochastic one.

The following statements formalize the main properties of Algorithm 2:

⁷ In general the function $\mathcal{H}(\mathbf{x})$ must be differentiable and strictly concave on a closed convex set S . The latter must include the feasible set $\{\mathbf{x} \geq 0 \mid A\mathbf{x} = \mathbf{b}\}$ of the problem as well as the unconstrained optimum of its objective $\langle \mathbf{c}, \mathbf{x} \rangle + T\mathcal{H}(\mathbf{x})$, that must belong to the interior of S , see [4] for details.

Algorithm 3: Bregman method in log domain.

1 **while** stopping criterion not fulfilled **do**

 // loop over cliques:

2 **for** $j \in [m]$ **do**

 // make the largest cost in the clique ≈ 0

3 $i^* \in \arg \max_{i \in \tilde{K}_j} c_i^\lambda$

4 $\lambda_j := \lambda_j + c_{i^*}^\lambda + T \log \sum_{i \in \tilde{K}_j} \exp \frac{c_i^\lambda - c_{i^*}^\lambda}{T}$

Result: λ

Lemma 1. After the first outer iteration of Algorithm 2 it holds $\mathbf{0} \leq \mathbf{x} \leq \mathbf{1}$.

Proposition 5. Iterates of Algorithm 2 converge to the solution of the smoothed clique cover relaxation (16).

To be able to apply Algorithm 2 to the clique relaxation (3) one has to define *how to select the temperature T* as well as *how to deal with situations when $s = \sum_{i \in \tilde{K}_j} x_i$ is numerically equal to zero*. The latter may happen due to computation of $x_i = \exp(c_i/T)$ for low temperatures and negative costs, and triggers an error during division to s . We cover the second question first in Section 6 and get back to the first one in Section 7.

6 Numerics

Log-domain numerics. Consider Algorithm 3. Note that it differs from Algorithm 1 by the single term $T \log \sum_{i \in \tilde{K}_j} \exp \frac{c_i^\lambda - c_{i^*}^\lambda}{T}$ in the computation pipeline.

The following presentation recapitulates the well-known result for this type of algorithms in the optimal transport domain:

Lemma 2. Algorithm 3 is equivalent to Algorithm 2 through the transformation $\mathbf{x} = \exp(\mathbf{c}^\lambda/T)$.

Contrary to Algorithm 2, Algorithm 3 is numerically stable. Its stability follows from $c_i^\lambda - c_{i^*}^\lambda \leq 0$ and, therefore, $\exp \frac{c_i^\lambda - c_{i^*}^\lambda}{T} \in (0,1]$, and $c_{i^*}^\lambda - c_{i^*}^\lambda = 0$ implying $\sum_{i \in \tilde{K}_j} \exp \frac{c_i^\lambda - c_{i^*}^\lambda}{T} > 1$. The latter is sufficient to have a numerically stable logarithm computation.

Lemma 3. After the first iteration of Algorithm 3 the reduced costs \mathbf{c}^λ remain non-positive, e.g., $\mathbf{c}^\lambda \leq \mathbf{0}$.

Proposition 6. Algorithm 3 converges to the optimum of the dual smoothed clique cover relaxation problem

$$\min_{\lambda} \left[D^T(\lambda) := \sum_{j=1}^m \lambda_j + \max_{\mathbf{x} \in [0,1]^{n+m}} \left(\langle \mathbf{c}^\lambda, \mathbf{x} \rangle + T\mathcal{H}(\mathbf{x}) \right) \right], \quad (17)$$

and implements the coordinate minimization principle. In particular, D^T is convex differentiable and right after processing the clique $j \in [m]$ in Line 4 it holds $\frac{\partial D^T}{\partial \lambda_j} = 0$.

Propositions 5 and 6 imply that the dual iterates λ of Algorithm 3 determine the primal ones $\mathbf{x} = \exp(\mathbf{c}^\lambda/T)$ and the latter converge to the solution of the smoothed clique relaxation (16).

Along with the advantages such as numerical stability and possibility to estimate an upper bound due to the explicit computations of the dual iterates, Algorithm 3 has a major disadvantage: It has high computational cost due to extensive exponentiations. An alternative way to perform computations that allows to keep advantages of Algorithm 3 and avoid its disadvantages is reviewed in the following paragraph.

Exp-domain numerics with stabilization is represented by Algorithm 4. It keeps track of the exponentiated version $\alpha_j := \exp(-\lambda_j/T)$, $j \in [m]$, of the dual variables. Note that for any $j \in [m]$ and any $i \in \bar{K}_j$, it holds

$$\begin{aligned} x_i &= \exp(\mathbf{c}_i^\lambda/T) = \exp\left[\frac{1}{T}\left(c_i - \sum_{j' \in \bar{K}_j} \lambda_{j'}\right)\right] \\ &= \exp\left[\frac{1}{T}\left(c_i - \sum_{j' \in \bar{K}_j \setminus \{j\}} \lambda_{j'}\right)\right] \cdot \exp(-\lambda_j/T) \\ &= \exp\left[\frac{1}{T}\left(c_i - \sum_{j' \in \bar{K}_j \setminus \{j\}} \lambda_{j'}\right)\right] \cdot \alpha_j. \end{aligned} \quad (18)$$

So, x_i , where $i \in \bar{K}_j$, are proportional to α_j . Hence, instead of normalizing x_i , we can update α_j by dividing it by the normalization factor s , see Line 4. The main advantage of this approach is an explicit computation of the dual variables (up to the logarithm operation). Since computation of the normalizing factor s requires values of \mathbf{x} , we update \mathbf{x} directly as well, see Line 6.

As long as α remains close enough to 1 (Line 5, see Section 10 for the used values of the *stabilization threshold* τ_{stab}), this implies stable computations for α and \mathbf{x} (Lines 4 and 6). Should α become very large or very small (Line 5), the computations may get imprecise and, therefore, one switches to the expensive computations in the log-domain to stabilize them (Lines 8 to 11).

Note, however, that close to the optimum of the smoothed problem (16), and, therefore, feasibility of \mathbf{x} , computations in Algorithm 4 *do not require stabilization* as $s \approx 1$ and, hence, $\alpha \approx 1$ in this case. This emphasizes importance of the proper scheduling of the temperature parameter T as the latter influences the distance to the smoothed optimum. We consider this question in Section 7.

7 Smoothing/Temperature scheduling

The lower the temperature T is, the better the smoothed clique cover relaxation (16) approximates its non-smoothed counterpart (3), see [42]. Given a required

Algorithm 4: Stabilized Bregman method in exp-domain.

Input: $\alpha_j = 1, j \in [m]; x_i = \exp(\mathbf{c}_i^\lambda/T), i \in [n]$

```

1 while stopping criterion not fulfilled do
2   for  $j \in [m]$  do
3     // Compute sum over the clique
4      $s := \sum_{i \in \bar{K}_j} x_i$ 
5     // update exponentiated dual
6      $\alpha_j := \alpha_j/s$ 
7     if  $\alpha_j + 1/\alpha_j < \tau_{\text{stab}}$  then
8       // if  $\alpha_j \approx 1$  run naive Bregman method
9        $x_i := x_i/s, \forall i \in \bar{K}_j$ 
10    else
11      // stabilize:
12      // push  $\alpha$  into  $\lambda$  to obtain a dual
13      // solution
14      for  $j \in [m]$  do
15         $\lambda_j := \lambda_j - T \log \alpha_j$ 
16         $\alpha_j := 1$  // reinitialize  $\alpha$ 
17      // update  $\mathbf{x}$  in a stable way
18       $x_i := \exp(\mathbf{c}_i^\lambda/T), \forall i \in \bar{K}_j$ 
19    // push  $\alpha$  into  $\lambda$  to obtain a dual solution
20  for  $j \in [m]$  do
21     $\lambda_j := \lambda_j - T \log \alpha_j$ 

```

Result: (\mathbf{x}, λ)

approximation level, one could imagine two strategies of temperature selection. The first one is the *fixed* temperature. Although being very simple, it leads to very slow algorithms. First, because the Bregman algorithm makes only small progress for low temperatures. Second, because the numerical stabilization in Algorithm 4 can be required very often for computations far from the optimum. This would eliminate the speed advantage of the exp-domain-based Algorithm 4 over the log-domain-based Algorithm 3.

Hence, a practical solution is the *temperature scheduling*, i.e., starting with a high value of T and decreasing it as the computation progresses. We consider two methods for the temperature scheduling below.

7.1 Method 1: Feasibility-based

Feasibility constraints satisfaction is the standard stopping criterion in the optimal transport literature [36], used to decide whether it is time to decrease the temperature. Typically, one checks whether

$$\left| \sum_{i \in \bar{K}_j} x_i - 1 \right| \leq \tau_{\text{feas}}, \forall j \in [m], \quad (19)$$

for some predefined *feasibility threshold* $\tau_{\text{feas}} \geq 0$. Should the constraints (19) be fulfilled, one drops the temperature by the predefined factor $0 < \tau_{\text{drop}} < 1$, i.e.

$T := \tau_{\text{drop}} \cdot T$. For higher efficiency the conditions (19) are checked only each $\tau_{\text{batch}} \in \mathbb{N}$ iterations.

Remark 2. To simplify the selection of the initial temperature and keep computations numerically stable, we

(i) Run one iteration of Algorithm 1 at the beginning to ensure $\mathbf{c}^\lambda < 0$, and

(ii) scale all costs such that they lie in the interval $[-1, 0]$.

After completing these operations, we launch Algorithm 4 with an initial temperature of $T = 0.01$.

Remark 3. There is an alternative method for feasibility-based temperature scheduling, introduced in [21] for the quadratic assignment problem and equivalent to the above rule with $\tau_{\text{drop}} = 0.5$. Although authors report its numerical stability in their experiments, for other problem instances it may require stabilization as well.

7.2 Method 2: Duality gap-based

Duality gap is an alternative way to control the distance to the optimum when dual variables λ are computed explicitly, i.e., in Algorithms 3 and 4. Let $\hat{\mathbf{x}}$ and \mathbf{x}^* be a feasible and an optimal solutions to the smoothed clique cover relaxation (16) respectively. Let also λ and λ^* be a feasible and an optimal solutions to its smoothed dual (17). The strong duality implies $\langle \mathbf{c}, \hat{\mathbf{x}} \rangle + T \mathcal{H}(\hat{\mathbf{x}}) \leq \langle \mathbf{c}, \mathbf{x}^* \rangle + T \mathcal{H}(\mathbf{x}^*) = D^T(\lambda^*) \leq D^T(\lambda)$. A progress of the Bregman method is assured if the inequalities above hold strictly, i.e., $T < \frac{D^T(\lambda) - \langle \mathbf{c}, \hat{\mathbf{x}} \rangle}{\mathcal{H}(\hat{\mathbf{x}})}$. This inequality turns into equality in the optimum of the smoothed problems (16)-(17). Hence, the respective temperature update condition, for a suitable predefined $0 < \tau_{\text{gap}} < 1$, may look like

$$\text{if } T > \tau_{\text{gap}} \frac{D^T(\lambda) - \langle \mathbf{c}, \hat{\mathbf{x}} \rangle}{\mathcal{H}(\hat{\mathbf{x}})} \text{ update } T. \quad (20)$$

To ensure monotonicity of the temperature, we update it by setting to

$$T := \min \left\{ T, \tau_{\text{gap}} \frac{D^T(\lambda) - \langle \mathbf{c}, \hat{\mathbf{x}} \rangle}{\mathcal{H}(\hat{\mathbf{x}})} \right\} \quad (21)$$

each $\tau_{\text{batch}} \in \mathbb{N}$ iterations. Between temperature changes Algorithm 3, or 4 is used.

7.3 Feasible primal estimates for Method 2

Obtaining feasible primal estimates. Let C stand for the feasible set of (16). Computations (20) and (21) require a feasible $\hat{\mathbf{x}}$, i.e., $\hat{\mathbf{x}} \in C$. Contrary to the unconstrained dual iterates λ , their primal counterparts $\mathbf{x} = \exp(\mathbf{c}^\lambda/T)$ are infeasible until convergence, i.e., $\mathbf{x} \notin C$. To obtain feasible iterates we project \mathbf{x} to the set C :

Definition 1. A mapping $\mathcal{P}: \mathbb{R}_{\geq 0}^{n+m} \rightarrow C$ is called projection, if it is idempotent, i.e., $\mathcal{P}(\mathcal{P}(\mathbf{x})) = \mathcal{P}(\mathbf{x})$, and continuous. The latter, in particular, guarantees that $\mathbf{x}^t \xrightarrow{t \rightarrow \infty} \mathbf{y} \in C$ implies $\mathcal{P}(\mathbf{x}^t) \xrightarrow{t \rightarrow \infty} \mathcal{P}(\mathbf{y}) = \mathbf{y}$.

Algorithm 5: Truncation projection.

Input: $\mathbf{x} \in \mathbb{R}_+^{n+m}$

// Initialize the feasible solution:

```

1  $\hat{\mathbf{x}} := \mathbf{0} \in \mathbb{R}^{n+m}$  // set all coordinates to 0 and
  // set slack variables to 1 for all  $m$  cliques:
2  $\hat{x}_{n+j} = 1, j \in [m]$ 
  // Update all non-slack variables:
3 for  $i \in [n]$  do
  // max. value of  $x_i$  fitting clique constraints:
4  $M := \min_{j \in J_i} \hat{x}_{n+j}$ 
5  $\hat{x}_i := \min\{x_i, M\}$  // truncate  $x_i$  if needed
6 for  $j \in J_i$  do
7    $\hat{x}_{n+j} := \hat{x}_{n+j} - \hat{x}_i$  // decrease the slacks resp.
```

Result: $\mathcal{P}(\mathbf{x}) := \hat{\mathbf{x}}$

Consider Algorithm 5 that introduces what we call a *truncation projection*. The algorithm checks all coordinates of \mathbf{x} and fixes their values in the projection $\hat{\mathbf{x}}$ as long as they do not violate the clique constraints. The value is truncated if necessary to avoid constraint violation. The slack variables \hat{x}_{n+j} are set to guarantee equality in the clique constraints.

Algorithm 5 has the following properties:

Lemma 4 (Feasibility). *The vector $\hat{\mathbf{x}}$ is always feasible at the end of each iteration of the outer loop defined in Line 3.*

Lemma 5 (Idempotence). *If the input \mathbf{x} is feasible, then $\mathcal{P}(\mathbf{x}) = \mathbf{x}$.*

Lemma 6 (Continuity). *The mapping $\mathcal{P}: \mathbb{R}_{\geq 0}^{n+m} \rightarrow C$ is continuous. Moreover,*

$$\left| \sum_{i \in \bar{K}_j} x_i - 1 \right| \leq \epsilon, \quad \forall j \in [m]. \quad (22)$$

implies

$$|x_i - \mathcal{P}(\mathbf{x})_i| \leq \epsilon, \quad \forall i \in [n]. \quad (23)$$

Lemmas 4 to 6 trivially result in

Theorem 1. *Mapping $\mathcal{P}(\mathbf{x})$ defined by Algorithm 5 is a projection to C .*

8 Sparsity-based speedup

As the temperature gets lower, the majority of values of the primal solution $\mathbf{x} = \exp(\mathbf{c}^\lambda/T)$ get closer to zero exponentially fast. Their influence on the value of the sum $s = \sum_{i \in \bar{K}_j} x_i$ of all variables in a given clique reduces accordingly, see Line 3 in Algorithm 4. Respectively, most of them can be completely ignored during computation to speed-up the latter. Below we consider two methods making use of this observation.

Heuristic truncation. In our first method we excluded from the summation all variables in a given clique if their values were at least a factor 10^{-8} smaller than the largest element in the clique. This reduced the efficient size of the cliques up to 10 times leading to significant speedup.

However, such a heuristic speedup may lead to an uncontrolled increase of the smoothed dual value D^T ruining algorithms convergence. This behavior is well-known in the optimal transport domain, see [35, Example 3.5]. Hence, below we derive a method that takes this issue into account.

Truncation based on a bounded dual perturbation (accurate truncation). Similarly to [36], our *accurate truncation* is based on the stabilization technique that guarantees a limited maximum value of the exponentiated dual variables α , see Algorithm 4. Contrary to [36], we compute the allowed truncation value based on the recent improvement of the smoothed dual value D^T instead of the primal-dual gap.

To this end consider the following statement:

Lemma 7. *For any $T \geq 0$ and $\mathbf{c} \leq 0$ it holds:*

$$\max_{\mathbf{x} \in [0,1]^{n+m}} (\langle \mathbf{c}, \mathbf{x} \rangle + T\mathcal{H}(\mathbf{x})) = T \sum_{i=1}^{n+m} \exp(c_i/T). \quad (24)$$

According to Lemma 7 the dual value D^T is equal to

$$\begin{aligned} D^T(\lambda) &= \sum_{j=1}^m \lambda_j + T \sum_{i=1}^{n+m} \exp(c_i/T) \prod_{j \in J_i} \exp(-\lambda_j/T) \\ &= \sum_{j=1}^m \lambda_j + T \sum_{i=1}^{n+m} x_i \prod_{j \in J_i} \alpha_j. \end{aligned} \quad (25)$$

Consider the truncated primal estimates

$$\bar{x}_i = \begin{cases} 0, & \text{if } x_i < \epsilon_i, \\ x_i, & \text{otherwise} \end{cases} \quad (26)$$

and the respective smoothed dual value

$$\bar{D}(\lambda) := \sum_{j=1}^m \lambda_j + T \sum_{i=1}^{n+m} \bar{x}_i \prod_{j \in J_i} \alpha_j. \quad (27)$$

Let δ be a maximum error in computation of D^T allowed due to truncation:

$$\begin{aligned} \delta &:= D^T(\lambda) - \bar{D}(\lambda) = T \sum_{i=1}^{n+m} (x_i - \bar{x}_i) \prod_{j \in J_i} \alpha_j \\ &\leq T \sum_{i=1}^{n+m} \epsilon_i \prod_{j \in J_i} \tau_{\text{stab}} = T \sum_{i=1}^{n+m} \epsilon_i \tau_{\text{stab}}^{|J_i|}. \end{aligned} \quad (28)$$

Algorithm 6: Greedy solution generation.

Input: $\mathbf{c}^\lambda \in \mathbb{R}^{n+m}$ // reduced costs
1 $\mathbf{x} := -\mathbf{1} \in \mathbb{R}^{n+m}$ // initialize \mathbf{x} as undefined
// iterate over all cliques in random order
2 **for** $j \in \text{shuffle}([m])$ **do**
// skip cliques with set nodes
3 **if** $\{i \in \bar{K}_j \mid x_i = 1\} = \emptyset$ **then**
// find assignable & locally optimal node
4 $i^* := \arg \max_{i \in \bar{K}_j \text{ s.t. } x_i = -1} c_i^\lambda$
5 $x_{i^*} := 1$ // set it to one
// and all its graph neighbors to zero:
6 **for** $i: \{i^*, i\} \in \mathcal{E}$ **do**
7 $x_i := 0$

Result: \mathbf{x}

Hence, setting

$$\epsilon_i \leq \frac{\delta}{T(n+m)\tau_{\text{stab}}^{|J_i|}} \quad (29)$$

guarantees that the truncation error in computation of the smoothed dual value does not exceed δ . In our experiments we set δ to 0.1 of the smoothed dual value improvement attained in the previous computation batch.

9 Simple primal heuristic

Although the primary subject of our work is the dual optimization, we have implemented a simple primal heuristic to be able to compare to existing methods that return solutions of the non-relaxed MWIS problem. Our primal heuristic consists of two iteratively repeating steps: (i) A randomized *greedy* feasible solution *proposal generation* and (ii) its *optimized recombination* with the best found solution so far.

Our greedy proposal generation step makes use of the dual optimization by being applied to the problem with the reduced costs \mathbf{c}^λ instead of the original ones \mathbf{c} .

The pseudo-code of the generation step is represented by Algorithm 6. It considers a graph with additional nodes, one per clique, corresponding to the slack variables introduced in (3). The algorithm randomly selects a yet unprocessed clique and adds the node with the lowest cost in the clique to the solution proposal. This node and all adjacent nodes are removed from the graph. The process is repeated until no nodes are left.

The optimal recombination (also known as crossover or fusion) step solves the MWIS problem (1) only for those variables whose values *differ* in the best integer solution found so far and in the newly generated solution proposal. The values of all other variables are fixed to

the values in best integer solution found so far. It is known [10] that such optimal recombination problem is reducible in linear time to the min-st-cut/max-flow and is efficiently and exactly solvable therefore. Instead, we opted for reducing it to a special form of the quadratic pseudo-boolean maximization problem (see Section 13), which can itself be efficiently solved via min-st-cut. This alternative approach was used since our implementation relies on software [32] that requires the quadratic pseudo-boolean function as input.

A similar primal algorithm for the MWIS problem has been proposed, e.g., in [7]. However, it uses (i) a different proposal generation, as explained in the following paragraph, and (ii) multiple local search algorithms applied to each generated solution proposal prior to recombination.

Related work on proposal generation Algorithm 6 resembles the WG algorithm of [18, Thm. 3] that works with non-negative costs. Let δ_i be the node degree. The WG algorithm iteratively and greedily adds to the solution the node $i^* = \arg \max_{i \in V} c_i / \delta_i$ and removes it and its neighbors from the graph. Hence, node degrees change on each step of the algorithm, and one has to maintain a priority queue, that slows down the algorithm. To speed up computations, this generation method is used to generate only the very first feasible solution proposal in [7]. For further solution proposals the changes in the node degrees during generation are not taken into account.

Our proposal generation is much faster than the WG algorithm, since we do not take the node degrees and their respective changes into account. Importantly, as the dual iterates λ get closer to the dual optimum, our algorithm becomes closer to the WG algorithm. This is because the optimal cost within each clique gets nearly zero (cf. Algorithm 3), just like its weighted degree c_i / δ_i .

9.1 Discussion: Usage of the relaxed solution.

As mentioned above, our primal heuristic profits from the relaxation optimization by employing the reduced costs \mathbf{c}^λ instead of the original ones \mathbf{c} . The work [7] instead uses the relaxed primal solution $\mathbf{x} \in [0, 1]^n$ in the local search procedure by arguing that “a node with a high value in the relaxed solution is more likely to be part of a good solution to the MWIS”. This argument, however, has no theoretical support for the clique cover relaxation. As follows from Proposition 4, all non-zero fractional-valued coordinates of the optimal primal solution \mathbf{x} correspond to zero reduced costs.⁸ Conversely, nodes whose reduced costs are lower than zero correspond to

zero-valued coordinates of the optimal primal relaxed solution, regardless of the actual cost values. Therefore, we argue that these are the reduced costs that contain essential information about LP relaxation that can be used in primal heuristics and not the primal relaxed solutions themselves. Although authors of [7] report improvement of their local search due to usage of the primal LP solution, we suspect that the main information which turns to be useful for their algorithm, is distinguishing between zero and non-zero primal LP values, and, respectively, zero- and non-zero reduced costs. Yet, should the usage of the primal relaxed solutions be preferable for any reason, our truncation projection Algorithm 5 provides their estimates even before the dual algorithm reaches the optimum.

Unfortunately, in case of the MWIS problem, the usage of the reduced costs has also disadvantages. That is, our reduced costs describe the modified problem (3). Although many primal heuristics can be adjusted to cope with this modification, this adjustment is critical for them to function properly. For example, reduced costs are non-positive and any sensible MWIS algorithm ignores nodes with non-positive costs as there is always an optimal solution consisting of nodes with positive costs only.

10 Experimental evaluation

Datasets. In our evaluation, we focus on large-scale, real-world MWIS problems. This approach contrasts with prior studies that primarily utilized augmented unweighted instances by assigning artificial randomized weights to the graph nodes [22]. There are two problems with the latter: (i) The variability in random weights across these studies complicates direct comparisons, and (ii) the use of random weights raises questions about the generalization of results to real-world applications. Moreover, even usage of existing non-randomly weighted graphs as a test bed for algorithms (cf. [13]) raises the question of practical usefulness, unless such problems have particular applicability in real-world scenarios.

All datasets we consider are readily represented as clique graphs, so we reuse these cliques in our algorithms.

Amazon Vehicle Routing [9]. These instances are derived from real-world long-haul vehicle routing problems at Amazon [1]. This dataset contains by far the largest MWIS instances which are publicly available, see Table 1. In each of the problems the nodes describe a set of routes and the cliques describe conflicts between them based on shared drivers or loads. We split this datasets into three subsets, with small (*AVR-small*), medium (*AVR-medium*) and large (*AVR-large*) problem instances, see Table 1 for details.

Meta-Segmentation for Cell Detection (MSCD) This dataset is derived from semi-automated labeling prob-

⁸ In fact, in multiple duality-based algorithms such as ours or, e.g., the primal simplex algorithm, the optimal reduced costs are non-positive. So, all non-zero coordinates of \mathbf{x} correspond to zero-valued reduced costs.

dataset	# instances	# nodes	# edges	# cliques	avg. clique size
AVR-large	17	127 k – 882 k	43 M – 344 M	5.4 k – 38 k	120.2
AVR-medium	16	10 k – 84 k	126 k – 39 M	1.8 k – 48 k	24.4
AVR-small	5	979 – 14 k	2.4 k – 44 k	805 – 15 k	3.2
MSCD	21	5 k – 8 k	66 k – 198 k	22 k – 36 k	8.8

Table 1: Datasets used for evaluation. We split the *AVR* dataset into *AVR-small*, *AVR-medium* and *AVR-large* based on the number of nodes. Here **#nodes** and **#edges** stand for the number of nodes and edges in the graph representation of the problem respectively, **#cliques** gives the number of clique constraints in the respective ILP representation (2), and **avg. clique size** is the average clique size per instance averaged over the number of instances in the dataset.

lems for cell segmentations [28, Ch. 7] and has been kindly provided by the author of [28]. We make this real-world MWIS dataset publicly available for usage by other researchers⁹. In each instance the nodes represent segmentations that are generated by multiple algorithms and, therefore, overlap with each other. The MWIS problem consists in selecting their non-overlapping subset with the minimal total cost (maximal total weight). The size of the instances from this datasets lies between *AVR-medium* and *AVR-small*, see Table 1.

Algorithms. We compare our method to the following solvers:

- *LP-Gurobi simplex/barrier* – Gurobi optimizer [15] in single-threaded LP mode with simplex or barrier method respectively. The problem formulation corresponds to the LP relaxation of the clique cover formulation (2). We lowered the optimality gap setting to zero to not let Gurobi exit prematurely. Apart from that the default parameters are used.
- *ILP-Gurobi barrier* – Gurobi optimizer [15] in single-threaded ILP mode with the barrier method used to compute the basic relaxation respectively. The barrier method is chosen as it leads to faster results for large problem instances. The addressed ILP problem is (2).
- *KaMIS branch & reduce/reduce & local-search* – Authors of the KaMIS framework [22] claim their state-of-the-art performance on large-scale MWIS problem instances, therefore we selected them as a representative of dedicated optimization techniques. The framework addresses MWIS problems with reduction rules and branching on variables (*branch & reduce*), or by running a local search method after an initial reduction (*reduce & local-search*). Both variants are used with default parameters.
- *KaMIS local-search only* – a representative of the local search paradigm for MWIS solvers. We obtained it by disabling the reduction code.

- *METAMIS* [7], *METAMIS+LP* [7], *ILSVND* [25] – recent primal MWIS heuristics. In contrast to other algorithms, we did not execute these methods ourselves due to the lack of available source code. Instead, we compare our results with those presented in [7].

All experiments were run on an Intel Core i7-4770 CPU (3.40 GHz) with wall-clock time measurements. To reduce the influence of background processes we run each experiment 6 times and report the best run.

Ablation study for the LP relaxation (Figure 1(a)). On the *AVR-medium* dataset we compare performance of Algorithms 1, 3 and 4 with both *feasibility* and *dual gap scheduling* (Sections 7.1 and 7.2 resp.) with *heuristic* or *accurate truncation* (Section 8) and without it.

We run all algorithms in LP mode, without the primal heuristic. The primal bound for them is computed with Algorithm 5. All algorithms use the same parameter values, where applicable: $\tau_{\text{batch}} = 50$, $\tau_{\text{drop}} = 0.5$, $\tau_{\text{feas}} = 0.01$, $\tau_{\text{gap}} = 0.5$, starting temperature $T = 0.01$. All algorithms but those that utilize *accurate speedup* use $\tau_{\text{stab}} = 10^{30}$, otherwise $\tau_{\text{stab}} = 10$ to allow for an efficient truncation according to (29).

For comparison, we provide primal-dual convergence plots averaged over all instances in the dataset. Due to similarity of the instances the averaged plot looks qualitatively similar to individual plots for each problem instance within dataset. Other datasets yield averaged plots qualitatively similar to Figure 1(a), thus we omit them here.

The dual bound corresponding to the edge relaxation is presented as a baseline (dotted horizontal line). This baseline proved very loose across *all* datasets, see Figure 1(b-e). On average, these solutions had 95 % fractional values (the median value is even 99.4 %), which prevents leveraging the persistency property to significantly reduce graph sizes.

The second baseline is given by the non-smoothed dual coordinate descent of Algorithm 1. Although its attained bound is much better than those of the edge relaxation, it is still very much inferior to the bounds attained by the other algorithms.

As expected, switching from *log*- to *exp*-domain (i.e., from Algorithm 3 to Algorithm 4) results in significant

⁹ See <https://vislearn.github.io/libmopt/mwis2025/>.

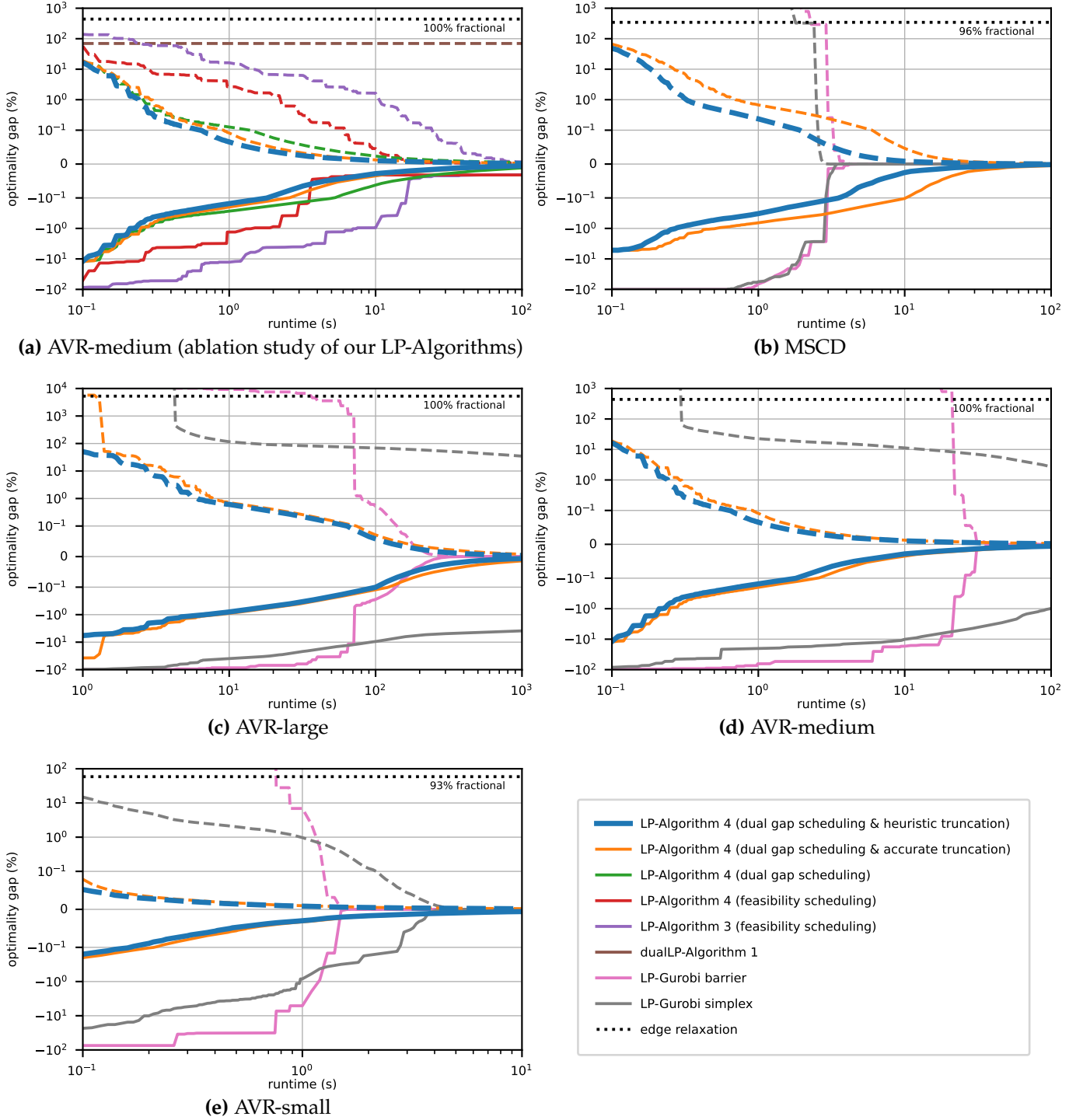


Figure 1: Optimization of the problem relaxation. These plots track the relative gap to the optimum of the LP relaxation of the MWIS problem (2) across runtime. Dashed lines refer to the dual objective (upper bound) and solid lines refer to the primal (relaxed) objective (lower bound). Instead of individual models, we show the mean objective across all models of the dataset group, providing a consolidated view of algorithm performance. Our algorithms are able to provide high-quality solutions ($< 1\%$ rel. gap) for the majority of the instances within 1–10 seconds.

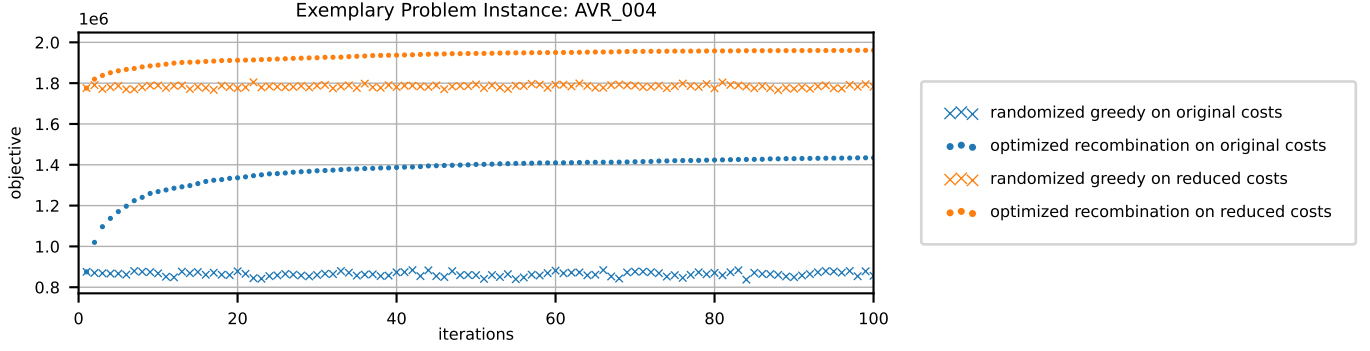


Figure 2: Primal heuristic ablation. Exemplary comparison on the problem instance *AVR_004* from the *AVR-large* dataset. As the comparison suggests, optimized recombination leads to significant improvement of the resulting solution. Even more improvement is obtained due to usage of the reduced costs: Even the best recombination result obtained for the original costs is worse than each single greedily generated solution based on reduced costs.

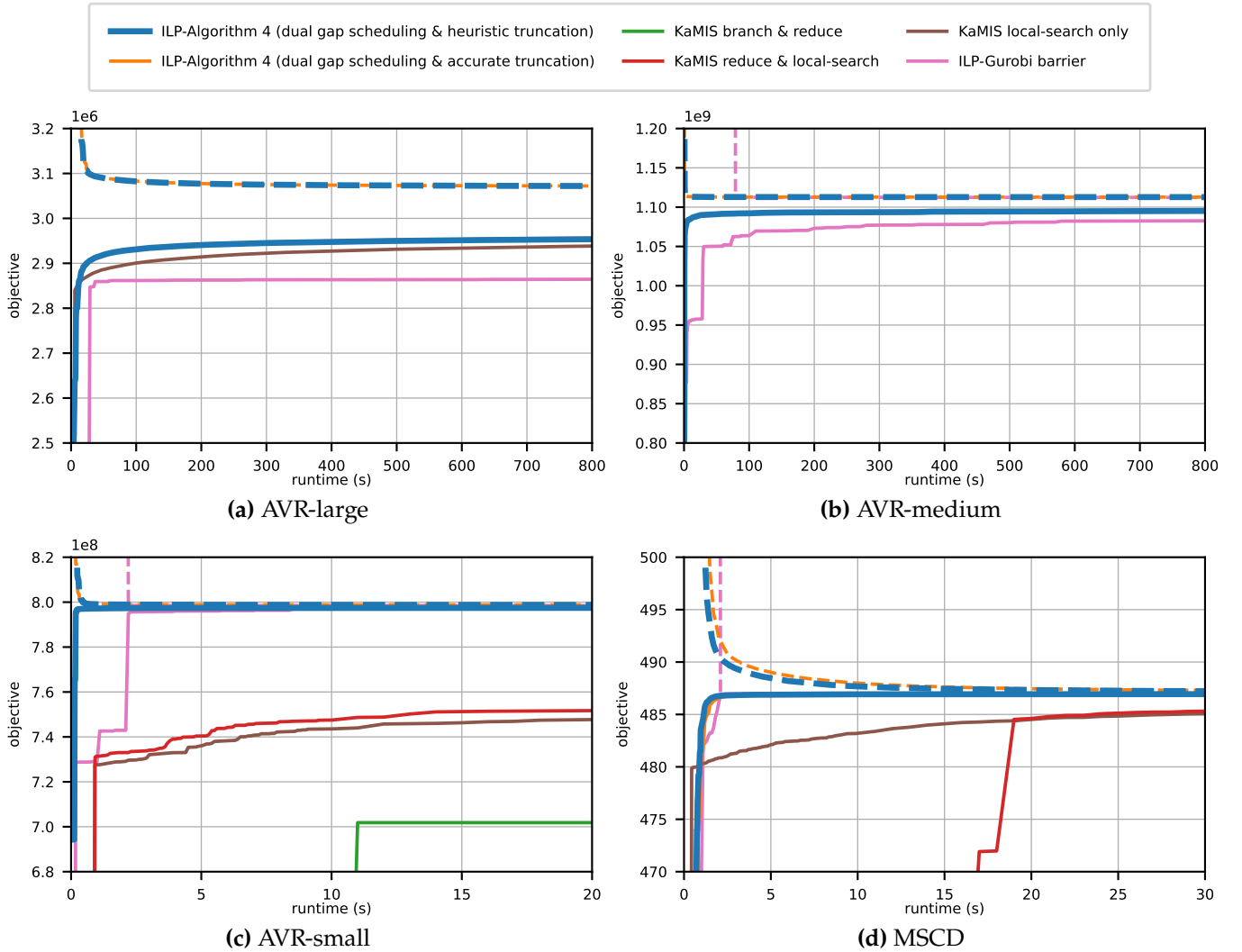


Figure 3: Optimization of the non-relaxed problem. This plot presents the absolute primal objective values over runtime, highlighting the effectiveness of our best-performing dual optimizer in conjunction with the proposed primal heuristics. Dashed lines refer to the dual objective (upper bound) and solid lines refer to the primal objective (lower bound). We compare our solver to *Gurobi* ILP and *KaMIS*. Similarly to Figure 1 we show the mean objective across all models of the different groups. Our solver yields high-quality MWIS solutions after only a few seconds for the majority of instances. Several variants of the *KaMIS* algorithms are missing in some plots as their attained values lie outside the visible area of the respective plots.

speedup in the range of almost an order of magnitude. Switching from *feasibility-* to *dual gap scheduling* (see Section 7) yields further significant speedups. For feasibility scheduling, we employed a relatively small threshold value τ_{feas} since larger values hinder convergence to the relaxed optimum. This occurs because the suboptimal starting point following a temperature drop leads to extremely slow convergence (numerically no convergence) at lower temperatures. In contrast, dual gap scheduling adjusts the temperature dynamically based on solution accuracy.

Finally, both *heuristic* and *accurate truncations* bring another speed-up to the whole algorithm. In total, Algorithm 4 with duality gap scheduling and heuristic or accurate truncation are our two best method and we use them in other experiments with the same parameters as above.

Our best methods against Gurobi in LP mode (Figure 1(b-e)). Our next experiment compares performance of Algorithm 4 with duality gap scheduling and heuristic/accurate truncation against *Gurobi simplex/barrier*. We do this with the same averaged plots as Figure 1(a).

The plots show that our methods significantly outperform *Gurobi* at the early optimization stages, but require much longer than *LP-Gurobi barrier* if a high accuracy is required. This is, however, a standard behavior of all first order methods including ours, due to their in total sub-linear (more precisely, exponentially low) convergence rate.

Although Algorithm 4 with *heuristic truncation* is always somewhat faster than with the *accurate truncation*, the difference is negligible in all datasets but *MSCD*. This is because instances of this datasets require stabilization more often, especially, when the relatively small stabilization threshold $\tau_{\text{stab}} = 10$ (see Algorithm 4) is used, as this is the case for the *accurate truncation*. This is the reason why we use the much higher value $\tau_{\text{stab}} = 10^{30}$ for all other algorithms.

Notably, *LP-Gurobi barrier* significantly outperforms *LP-Gurobi simplex* on all datasets but *MSCD* (for the latter their performance is comparable), hence we stick to *LP-Gurobi barrier* for our later experiments in the ILP mode.

Ablation study for our primal heuristic (Figure 2). In our third experiment we show importance of the optimized recombination and usage of the reduced costs instead of the original ones. This phenomenon is not unique to this specific example and similar results can be observed for most problem instances.

As shown in Figure 2, optimized recombination leads to a significant improvement of the resulting solution. Even more improvement is obtained due to the usage of the reduced costs: Even the best recombination result

obtained for the original costs is worse than each single greedily generated solution based on reduced costs.

Our best methods against competitors in ILP mode (Figure 3). In this experiment, we compare different methods addressing the *non-relaxed* MWIS problem (2). As with Figure 1, we show averaged plots and state their qualitative similarity to individual plots within each dataset. From our algorithms we show only Algorithm 4 with duality gap scheduling and heuristic/accurate truncation, where additionally 50 integer solution proposals are generated with Algorithm 6 each $\tau_{\text{batch}} = 50$ dual iterations and sequentially recombined with the current best integer solution.

In the short run our algorithms outperforms all its competitors on all datasets but *MSCD*, where the results in terms of the primal integer solution are on par with *ILP-Gurobi barrier*. In general *ILP-Gurobi barrier* is the most competitive among other methods. Only *KaMIS local search only* was able to show better results and only for the *AVR-large* dataset. On all other datasets, each of the three tested *KaMIS* variants is noncompetitive, at least in the considered time span of 800 seconds.

On the small-sized datasets *AVR-small* and *MSCD* the comparison between our Algorithm 4 and *ILP-Gurobi barrier* leads to similar results as for the comparison in the LP mode, see Figure 1. Specifically, our method is faster initially, quickly finds a good approximate solution, but does not converge to the ILP optimum. In contrast, *ILP-Gurobi barrier* starts slightly slower but eventually finds the ILP optimum.

However, for larger datasets *AVR-large* and *AVR-medium* *ILP-Gurobi barrier* is not always able to find the optimum and often is even unable to reach the solution accuracy of our methods within 1 000 seconds.

This type of performance is typical when comparing exact methods like *ILP-Gurobi barrier* to approximate ones like ours. Our method performs well because the reduced costs from dual optimization give it a significant advantage early on. Being very important for the performance of the primal heuristic at the beginning, its effect diminishes as we approach the solution of the relaxed problem. In other words, primal heuristics generally cannot fully benefit from high-precision relaxed solutions, whereas Gurobi’s branch-and-bound method can.

Comparison to METAMIS [7] and ILSVND [25]. The comparison to these state-of-the-art primal heuristics on all three *AVR* datasets is given in Table 2. To this end, we follow the setting of [7]. We run the fastest variant of *Our* method, namely Algorithm 4 with our primal heuristic, duality gap scheduling and heuristic truncation, five times with different random seeds for 3 600 seconds. This matches the runtime used by the authors of [7] for their experiments. Like [7], we report the best result from each run for every problem instance.

Dataset	Instance	Our (3 600 sec)		“Cold” (c.f. [7, Tab. 2])		“Warm” (c.f. [7, Tab. 3])		
		Objective	time in s until LP-Gap 0.1 %	time in s to surpass ... ILSVND	time in s to surpass ... METAMIS	time in s to surpass ... ILSVND	time in s to surpass ... METAMIS	time in s to surpass ... METAMIS+LP
AVR-LARGE	CR-S-L-1	5 653 748	309	4	63	424	—	—
	CR-S-L-2	5 737 640	289	12	198	590	—	—
	CR-S-L-4	5 734 265	297	8	113	672	—	—
	CR-S-L-6	3 909 318	110	6	34	1 840	—	—
	CR-S-L-7	2 011 084	19	2	15	507	—	—
	CR-T-C-1	4 723 108	50	2	13	122	—	—
	CR-T-C-2	4 945 899	122	2	22	166	—	—
	CR-T-D-4	4 881 646	170	2	34	583	—	—
	CR-T-D-6	3 013 249	75	1	11	290	—	—
	CR-T-D-7	1 455 976	10	< 1	3	—	—	—
	CW-S-L-1	1 648 272	190	13	85	—	—	—
	CW-S-L-2	1 722 290	186	25	148	—	—	—
	CW-S-L-4	1 733 085	133	36	463	—	—	—
	CW-S-L-6	1 164 850	35	9	137	—	—	—
	CW-S-L-7	589 334	10	7	90	—	—	—
	CW-T-C-1	1 330 362	15	6	39	1 016	—	—
	CW-T-C-2	937 013	14	10	206	—	—	—
AVR-MEDIUM	CW-T-D-4	460 198	2	1	6	56	—	—
	CW-T-D-6	459 776	2	< 1	7	28	—	—
	MR-D-03	1 758 074 154	1	< 1	< 1	< 1	18	80
	MR-D-05	1 790 179 623	1	< 1	1	< 1	2	8
	MR-D-FN	1 802 268 039	1	< 1	1	< 1	3	8
	MR-W-FN	5 386 842 781	< 1	< 1	< 1	< 1	< 1	< 1
	MT-D-200	287 155 108	< 1	< 1	< 1	< 1	< 1	< 1
	MT-D-FN	<i>290 866 943</i>	< 1	< 1	165	< 1	< 1	< 1
	MT-W-200	384 056 012	< 1	< 1	< 1	< 1	< 1	< 1
	MT-W-FN	390 869 891	< 1	< 1	< 1	< 1	< 1	< 1
	MW-D-20	526 688 093	< 1	< 1	1	< 1	1	2
	MW-D-40	538 944 498	< 1	< 1	2	< 1	1	3
	MW-D-FN	545 720 496	< 1	< 1	< 1	< 1	4	6
	MW-W-05	1 329 653 408	18	1 699	1 699	1 699	1 699	1 699
	MW-W-10	<i>1 300 124 841</i>	18	—	—	—	—	—
	MW-W-FN	<i>1 248 553 336</i>	17	—	—	—	—	—
AVR-SMALL	MR-D-01	1 691 358 724	< 1	< 1	1	< 1	< 1	< 1
	MT-D-01	<i>238 166 485</i>	< 1	< 1	< 1	< 1	< 1	< 1
	MT-W-01	<i>312 121 568</i>	< 1	< 1	< 1	< 1	< 1	< 1
	MW-D-01	476 361 236	< 1	18	141	3	18	18
	MW-W-01	<i>1 270 305 952</i>	< 1	< 1	< 1	< 1	< 1	< 1
ALL		better objective: 32 equal objective: 4 worse objective: 2						

Table 2: Comparison of Algorithm 4 with our primal heuristic, duality gap scheduling and heuristic truncation denoted as *Our* to METAMIS [7] and ILSVND [25] based on [7, Tab. 2, 3]. All algorithms have been run for 3 600 seconds. Datasets are sorted by their size, from the largest on top to the smallest in the bottom. “Warm” and “Cold” columns correspond to competing algorithms that use or, respectively, do not use a warm-start with a specific (unpublished, unknown and not used by *Our*) initial solution as explained in [7]. **LP-Gap 0.1%** – time required to attain the 0.1% relative duality gap for the relaxed problem. **ILSVND, METAMIS, METAMIS+LP** – time required by *Our* algorithm to attain the best value of the respective competing method. This value is taken from the column “w” in [7, Tab. 2, 3]. To obtain the full time of *Our* algorithm its time should be added to the respective value in the “LP-Gap 0.1 %” column. Objective value marked as **bold** means that this is *strictly greater* than those obtained by any competing algorithm with the “Cold”-start. *Italic* font means that our value and value of the best competing algorithm coincide: For two of them, MT-D-01 and MT-W-01, this value furthermore coincides with the LP bound and is, therefore, optimal. Although *Our* method only uses a comparably simple primal heuristics, it outperforms its competitors due to the usage of the reduced costs, see a detailed explanation in the main text.

To separate runtime contribution of our dual method from those of the primal heuristic, we first run the dual updates until the 0.1% relative duality gap for the relaxed LP is attained and only afterwards start running primal heuristic in each batch additionally (50 solution proposals per batch). Typically, due to sparsity, the time needed by dual updates after attaining the above duality gap constitutes less than 5% of the time required by the primal heuristic and, therefore, can be largely ignored.

Table 2 shows the time required by our method to attain or exceed the results of the competing algorithms. Following [7], we evaluate the competing algorithms under both “cold” and “warm”-start conditions. The latter uses an unpublished, therefore, unknown and not used by our algorithm, initial solution. We refer to [7] for further details and actual objective values attained by the METAMIS and ILSVND algorithms.

As can be seen from Table 2, for all but two datasets (MW-W-10 and MW-W-FN) our method finds better or the same accuracy solutions as the competitors with “cold” start. For most of instances of *AVR-medium* and *AVR-small* this happens within 1 second, few require up to 7 seconds and only three instances – more than 100 seconds after attaining the 0.1% duality gap for the relaxed problem. Finding better solutions than METAMIS for instances from *AVR-large* requires less than 100 seconds for 11 problem instances of 17, and at most 206 seconds for each of the rest 6 instances. Note that according to [7], METAMIS as well as ILSVND failed to converge within 3 600 seconds “on larger instances” (we assume *AVR-large*) and essentially required that time to attain their best solutions. Additionally, our algorithm attains the best objective values of ILSVND significantly faster than METAMIS, c.f. [7][Tab. 2, column METAMIS- t^* [s]].

Moreover, Our method outperformed all competitors, even those that utilized a “warm”-start initial solution, for most of *AVR-medium* and *AVR-small* problem instances. Naturally, this warm-start solution, which was unpublished and unknown to us, was not included in Our algorithm. In the experiments of [7], this “warm”-start initial solution significantly enhanced the performance of both, METATMIS and ILSVND algorithms. Additionally, METATMIS+LP leverages the primal LP solution to guide its local search, in addition to using the initial solution.

The question arises: *Why does Our method outperform METAMIS, which employs a much stronger primal heuristic?* Our experiments suggests that usage of the reduced costs instead of original ones is the key factor influencing the outcome. This is clearly demonstrated for our primal heuristic in Figure 2. Unfortunately, as mentioned in Section 9.1, using our reduced costs with the MWIS problem requires adjustments to primal heuristics. Furthermore, some heuristics cannot even be used at all. These limitations prevented us from running KaMIS and ILSVND algorithms (the code of METAMIS is not pub-

lished) with our reduced costs to further substantiate our claim.

11 Conclusions

We presented a new method to address the maximum-weight independent set problem. The key component of the method is an approximate solver for the clique cover LP relaxation. Using reduced costs enables simplifying and speeding up the primal heuristic. This, in turn, leads to a competitive approximate solver of the non-relaxed problem. The advantages of our method are best seen on large-scale problem instances.

We expect our method to become even more competitive when used with more powerful primal heuristics that additionally include local search as a subroutine.

12 Acknowledgments

We thank Prof. Bernhard Schmitzer for an insightful discussion about modern advances in computational optimal transport. The discussion lead to the decisive speedup of our algorithms described in this work. A special thanks to Prof. Paul Swoboda for thorough proofreading and numerous comments that notably improved this paper. This work was supported by the German Research Foundation projects 498181230 and 539435352. Authors further acknowledge facilities for high throughput calculations bwHPC of the state of Baden-Württemberg (DFG grant INST 35/1597-1 FUGG) as well as Center for Information Services and High Performance Computing (ZIH) at TU Dresden.

References

- [1] Amazon. <http://www.amazon.com>.
- [2] Dimitri P. Bertsekas. Nonlinear programming, second edition. Athena scientific, 1999.
- [3] Endre Boros and Peter L. Hammer. Pseudo-boolean optimization. *Discrete applied mathematics*, 123(1-3):155–225, 2002.
- [4] Lev M. Bregman. The Relaxation Method of Finding the Common Point of Convex Sets and its Application to the Solution of Problems in Convex Programming. *USSR Computational Mathematics and Mathematical Physics*, 1967.
- [5] William Brendel and Sinisa Todorovic. Segmentation as maximum-weight independent set. In *Advances in Neural Information Processing Systems*, 2010.

- [6] Tomáš Dlask and Bogdan Savchynskyy. Relative-Interior Solution for (Incomplete) Linear Assignment Problem with Applications to Quadratic Assignment Problem. *arXiv preprint arXiv:2301.11201*, 2023.
- [7] Yuanyuan Dong, Andrew V. Goldberg, Alexander Noe, Nikos Parotsidis, Mauricio G.C. Resende, and Quico Spaen. A Local Search Algorithm for Large Maximum Weight Independent Set Problems. In *30th Annual European Symposium on Algorithms (ESA 2022)*. Schloss-Dagstuhl-Leibniz Zentrum für Informatik, 2022.
- [8] Yuanyuan Dong, Andrew V. Goldberg, Alexander Noe, Nikos Parotsidis, Mauricio G.C. Resende, and Quico Spaen. A metaheuristic algorithm for large maximum weight independent set problems. *arXiv preprint arXiv:2203.15805*, 2022.
- [9] Yuanyuan Dong, Andrew V. Goldberg, Alexander Noe, Nikos Parotsidis, Mauricio G.C. Resende, and Quico Spaen. New instances for maximum weight independent set from a vehicle routing application. In *Operations Research Forum*, volume 2, pages 1–6. Springer, 2021.
- [10] Anton Ereemeev and Julia Kovalenko. Optimal recombination in genetic algorithms for combinatorial optimization problems: Part I. *Yugoslav Journal of Operations Research*, 24(1):1–20, 2014.
- [11] Shu-Cherng Fang, Jay R. Rajasekera, and H.-S. Jacob Tsao. Entropy optimization and mathematical programming, volume 8. Springer Science & Business Media, 2012.
- [12] Michael R. Garey and David S. Johnson. Computers and intractability. W. H. Freeman and Company, New York, 1979.
- [13] Ernestine Großmann, Sebastian Lamm, Christian Schulz, and Darren Strash. Finding near-optimal weight independent sets at scale. In *Proceedings of the Genetic and Evolutionary Computation Conference*, pages 293–302, 2023.
- [14] Martin Grötschel, László Lovász, and Alexander Schrijver. Polynomial algorithms for perfect graphs. In *North-Holland mathematics studies*. Volume 88, pages 325–356. Elsevier, 1984.
- [15] Gurobi. Gurobi Optimization, 2018. <http://www.gurobi.com>.
- [16] Stefan Haller, Lorenz Feineis, Lisa Hutschenreiter, Florian Bernard, Carsten Rother, Dagmar Kainmüller, Paul Swoboda, and Bogdan Savchynskyy. A comparative study of graph matching algorithms in computer vision. In *European Conference on Computer Vision*, pages 636–653. Springer, 2022.
- [17] Dorit Hochbaum. Approximating covering and packing problems: set cover, vertex cover, independent set, and related problems. In *Approximation algorithms for NP-hard problems*, pages 94–143. 1996.
- [18] Akihisa Kako, Takao Ono, Tomio Hirata, and Magnús M. Halldórsson. Approximation algorithms for the weighted independent set problem. In *Graph-Theoretic Concepts in Computer Science: 31st International Workshop, WG 2005, Metz, France, June 23-25, 2005, Revised Selected Papers 31*, pages 341–350. Springer, 2005.
- [19] KaMIS - Karlsruhe Maximum Independent Sets. <https://karlsruhemis.github.io/>.
- [20] Richard M. Karp. Reducibility among combinatorial problems. In *Complexity of computer computations*. Springer, 1972.
- [21] Yam Kushinsky, Haggai Maron, Nadav Dym, and Yaron Lipman. Sinkhorn algorithm for lifted assignment problems. *SIAM Journal on Imaging Sciences*, 12(2):716–735, 2019.
- [22] Sebastian Lamm, Christian Schulz, Darren Strash, Robert Williger, and Huashuo Zhang. Exactly solving the maximum weight independent set problem on large real-world graphs. In *2019 Proceedings of the Twenty-First Workshop on Algorithm Engineering and Experiments (ALENEX)*, pages 144–158. SIAM, 2019.
- [23] John W. Moon and Leo Moser. On cliques in graphs. *Israel journal of Mathematics*, 3:23–28, 1965.
- [24] George L. Nemhauser and Leslie E. Trotter Jr. Vertex packings: Structural properties and algorithms. *Mathematical Programming*, 8(1):232–248, 1975.
- [25] Bruno Nogueira, Rian G.S. Pinheiro, and Anand Subramanian. A hybrid iterated local search heuristic for the maximum weight independent set problem. *Optimization Letters*, 12:567–583, 2018.
- [26] Vangelis T. Paschos. A survey of approximately optimal solutions to some covering and packing problems. *ACM Computing Surveys (CSUR)*, 29(2):171–209, 1997.
- [27] Gabriel Peyré, Marco Cuturi, et al. Computational optimal transport. *Center for Research in Economics and Statistics Working Papers*, (2017-86), 2017.
- [28] Mangal Prakash. Fully Unsupervised Image Denoising, Diversity Denoising and Image Segmentation with Limited Annotations. PhD thesis, Technische Universität Dresden, 2022.
- [29] Daniel Průša and Tomáš Werner. Solving LP relaxations of some NP-hard problems is as hard as solving any linear program. *SIAM Journal on Optimization*, 29(3):1745–1771, 2019.
- [30] Wayne Pullan. Optimisation of unweighted/weighted maximum independent sets and minimum vertex covers. *Discrete Optimization*, 6(2):214–219, 2009.

- [31] Elisabeth Rodriguez-Heck, Karl Stickler, Matthias Walter, and Stefan Weltge. Persistency of Linear Programming Formulations for the Stable Set Problem. *Mathematical programming*, 192:387–407, 1, 2022/3.
- [32] Carsten Rother, Vladimir Kolmogorov, Victor S. Lempitsky, and Martin Szummer. Optimizing Binary MRFs via Extended Roof Duality. In *Proceedings of the IEEE Conference on Computer Vision and Pattern Recognition*, 2007.
- [33] Sujay Sanghavi, Devavrat Shah, and Alan Willsky. Message passing for max-weight independent set. *Advances in Neural Information Processing Systems*, 20, 2007.
- [34] Bogdan Savchynskyy. Discrete Graphical Models – An Optimization Perspective. *Foundations and Trends in Computer Graphics and Vision*, 2019.
- [35] Bernhard Schmitzer. Stabilized sparse scaling algorithms for entropy regularized transport problems. *arXiv Preprint arXiv:1610.06519v1*, 2016.
- [36] Bernhard Schmitzer. Stabilized sparse scaling algorithms for entropy regularized transport problems. *SIAM Journal on Scientific Computing*, 41(3):A1443–A1481, 2019.
- [37] Alexander Schrijver. Combinatorial optimization: polyhedra and efficiency, volume 24 of number 2. Springer, 2003.
- [38] Devavrat Shah. Max product for max-weight independent set and matching. *arXiv preprint cs/0508097*, 2005.
- [39] Richard Sinkhorn. A Relationship Between Arbitrary Positive Matrices and Doubly Stochastic Matrices. *The Annals of Mathematical Statistics*, 1964.
- [40] Source code of algorithms for minimizing functions of binary variables with unary and pairwise terms based on roof duality by Vladimir Kolmogorov. <https://pub.ista.ac.at/~vnk/software/QPB0-v1.4.src.zip>.
- [41] Luca Trevisan. Inapproximability of combinatorial optimization problems. *Paradigms of Combinatorial Optimization: Problems and New Approaches*:381–434, 2014.
- [42] Jonathan Weed. An explicit analysis of the entropic penalty in linear programming. In *Conference On Learning Theory*, pages 1841–1855. PMLR, 2018.

13 Appendix

Transformation of the recombination problem (Section 9) into quadratic pseudo-boolean maximization

Let \mathcal{V}' stand for the set of graph nodes that differ in two feasible solutions $\mathbf{x}^1, \mathbf{x}^2 \in \{0, 1\}^n$ of the MWIS problem (1) to be fused, i.e., $x_i^1 = \bar{x}_i^2$, $i \in \mathcal{V}'$ and $x_i^1 = x_i^2$ for $i \in \mathcal{V} \setminus \mathcal{V}'$ respectively. Let \mathbf{c} be the cost vector of the problem. Let also the set of edges \mathcal{E}' be inherited from the initial problem: $\mathcal{E}' = \{\{i, j\} \in \mathcal{E} : i, j \in \mathcal{V}'\}$. By construction, the graph $(\mathcal{V}', \mathcal{E}')$ is bipartite, that is $\mathcal{E}' \subseteq \mathcal{V}^1 \times \mathcal{V}^2$, where $\mathcal{V}' = \mathcal{V}^1 \cup \mathcal{V}^2$, $\mathcal{V}^1 \cap \mathcal{V}^2 = \emptyset$, $\mathcal{V}^k = \{i \in \mathcal{V}' : x_i^k = 1\}$, $k = 1, 2$. For the sake of notation we assume the edges to be oriented, e.g., $(i, i') \in \mathcal{E}'$ implies $i \in \mathcal{V}^1$ and $i' \in \mathcal{V}^2$.

Consider the variable substitution

$$\forall i \in \mathcal{V}' : (y_i, w_i) := \begin{cases} (x_i, c_i), & i \in \mathcal{V}^1 \\ (\bar{x}_i, -c_i), & i \in \mathcal{V}^2. \end{cases} \quad (30)$$

Then for any $i \in \mathcal{V}^2$ and binary x_i it holds $c_i x_i = w_i y_i - w_i$. This turns the quadratic pseudo-boolean representation (5) of the considered MWIS problem into the so called *oriented form* [34, Ch. 11] as follows:

$$\begin{aligned} \sum_{i \in \mathcal{V}'} c_i x_i - M \cdot \sum_{(i,j) \in \mathcal{E}'} x_i x_j \\ = - \sum_{i \in \mathcal{V}^2} w_i + \sum_{i \in \mathcal{V}'} w_i y_i - M \cdot \sum_{(i,l) \in \mathcal{E}'} y_i \bar{y}_l. \end{aligned} \quad (31)$$

As shown in, e.g., in [34, Ch. 11], maximization of the right-hand-side of (31) reduces to the min-st-cut and we used the software [40] that implements this reduction and solves the respective min-st-cut problem.

Proof of Proposition 1. Due to half-integrality, it is sufficient to consider only half-integer feasible solutions. Due to the cost non-negativity the feasible solution $\mathbf{y} = (\underbrace{\frac{1}{2}, \frac{1}{2}, \dots, \frac{1}{2}}_n)$ is the best among those with coordi-

nates $1/2$ and 0 only, as it contains the maximal number of non-zero coordinates. The cost of this solution is $\langle \mathbf{c}, \mathbf{y} \rangle = \frac{1}{2} \sum_{j \in \mathcal{V}} c_j$.

Consider now feasible solutions that are at least one coordinate equal to 1 . Since the graph is fully-connected, there are only $|\mathcal{V}|$ of them, e.g., those of the form $\mathbf{x}^i = (\underbrace{0, \dots, 0}_{i-1}, 1, 0, \dots, 0)$ with the total costs equal to

c_i , respectively. The condition of the proposition implies

$$c_i < \sum_{j \in \mathcal{V} \setminus \{i\}} c_j = \sum_{j \in \mathcal{V}} c_j - c_i \quad (32)$$

and, therefore, $c_i < \frac{1}{2} \sum_{j \in \mathcal{V}} c_j = \langle \mathbf{c}, \mathbf{y} \rangle$. \square

Proof of Proposition 2. The proof is a direct consequence of the fact that for any $\mathbf{x} \in [0, 1]^n$ an inequality $\sum_{i \in K_l} x_i \leq 1$ implies $\sum_{i \in K'_j} x_i \leq 1$ as long as $K'_j \subseteq K_l$. \square

Proof of Proposition 3. It is sufficient to prove that the feasible set being a polytope has only integer vertices. Indeed, assume $\mathbf{x}' \in [0, 1]^n$ is a vertex. Then there is $\mathbf{c} \in \mathbb{R}^n$ such that \mathbf{x}' is a unique solution of $\{\max_{\mathbf{x} \in [0, 1]^n} \langle \mathbf{c}, \mathbf{x} \rangle, \text{ s.t. } \sum_{i=1}^n x_i \leq 1\}$. Assume that \mathbf{x}' is fractional and w.l.o.g. $c_1 \geq c_2 > 0$ and $x'_1, x'_2 > 0$. Then

$$\begin{aligned} \langle \mathbf{c}, \mathbf{x}' \rangle &= c_1 x'_1 + c_2 x'_2 + \sum_{i=3}^n c_i x'_i \\ &\leq c_1 (x'_1 + x'_2) + c_2 \cdot 0 + \sum_{i=3}^n c_i x'_i = \langle \mathbf{c}, \mathbf{x}'' \rangle, \end{aligned} \quad (33)$$

where \mathbf{x}'' such that $x''_1 = x'_1 + x'_2$, $x''_2 = 0$ and $x''_i = x'_i$ for $i = 3 \dots n$. \mathbf{x}'' is feasible since \mathbf{x}' is feasible as vertex. If the inequality in (33) holds strictly, then \mathbf{x}' is not a solution and if it holds as equality, then \mathbf{x}' is not a unique one. So we obtained a contradiction. \square

Proof of Proposition 4. The condition $\frac{\partial D}{\partial \lambda_j}[\mathbf{x}^*] = 0$ for all $j \in [m]$ together with (9) implies feasibility of \mathbf{x}^* and optimality of λ . Therefore, for any \mathbf{x} feasible for (3) it holds

$$\langle \mathbf{c}, \mathbf{x} \rangle \leq D(\lambda) = \sum_{j=1}^m \lambda_j + \langle \mathbf{c}^\lambda, \mathbf{x}^* \rangle = \langle \mathbf{c}, \mathbf{x}^* \rangle, \quad (34)$$

and thus, \mathbf{x}^* is an optimal solution of (3). If additionally \mathbf{x}^* is integer, inequality (34) proves its optimality for the non-relaxed problem (2) as well. \square

Proof of Lemma 1. The proof directly follows from the fact that every time the value of x_i , $i \in [n + m]$, changes, it is divided by a value $s \geq x_i$. \square

Proof of Proposition 5. Algorithm 2 is a special case of the algorithm that converges to the optimum of $\{\max_{\mathbf{x} \geq 0} \langle \mathbf{c}, \mathbf{x} \rangle + T\mathcal{H}(\mathbf{x}), \text{ s.t. } A\mathbf{x} = \mathbf{b}\}$ described in [4, pp. 215-216]. In particular:

- Initial value of \mathbf{x} is selected as an unconstrained maximum of the objective function. Indeed,

$$0 = (\langle \mathbf{c}, \mathbf{x} \rangle + T\mathcal{H}(\mathbf{x}))' = \mathbf{c} - T \log \mathbf{x}. \quad (35)$$

This implies $\mathbf{x} = \exp(\mathbf{c}/T)$.

- According to [4, Eq.(2.34), (2.35)], the update rule has a form

$$x'_i := x_i \exp(\gamma a_{ij}/T), \quad (36)$$

where γ is computed as a solution of

$$\sum_{i=1}^{n+m} a_{ij} x_i \exp(\gamma a_{ij}/T) = b_j. \quad (37)$$

Here the matrix $A = (a_{ij})$ and vector $\mathbf{b} = (b_j)$ define constraints $A\mathbf{x} = \mathbf{b}$ of the problem, i and j are the

column and row indices respectively. In our case $b_j = 1$ and $a_{ij} = \mathbb{I}[i \in \bar{K}_j]$, where $\mathbb{I}[B]$ is Iverson bracket equal to 1 if B holds, otherwise 0.

Plugging the values of a_{ij} and b_j into (36) and (37) and solving the latter w.r.t. γ leads to the update $x'_i = \frac{x_i}{\sum_{i \in \bar{K}_j} x_i}$.

□

Proof of Lemma 2. Indeed, let $\lambda'_k = \lambda_k$ for $k \neq j$ and

$$\begin{aligned} \lambda'_j &:= \lambda_j + c_i^\lambda + T \log \sum_{i \in \bar{K}_j} \exp \frac{c_i^\lambda - c_i^\lambda}{T} \\ &= \lambda_j + T \log \sum_{i \in \bar{K}_j} \exp(c_i^\lambda/T). \end{aligned} \quad (38)$$

Taking in account the transformation $\mathbf{x} = \exp(\mathbf{c}^\lambda/T)$, the elementary update in Algorithm 2 can be rewritten as

$$\begin{aligned} x'_i &:= \frac{x_i}{\sum_{i \in \bar{K}_j} x_i} = \frac{\exp(c_i^\lambda/T)}{\sum_{i \in \bar{K}_j} \exp(c_i^\lambda/T)} \\ &= \exp \left(\frac{c_i^\lambda - T \log \sum_{i \in \bar{K}_j} \exp(c_i^\lambda/T)}{T} \right) \\ &= \exp \left(\frac{c_i - \sum_{k \in J_i} \lambda_k - T \log \sum_{i \in \bar{K}_j} \exp(c_i^\lambda/T)}{T} \right) \\ &= \exp \left(\frac{c_i - \sum_{k \in J_i \setminus \{j\}} \lambda_k - (\lambda_j + T \log \sum_{i \in \bar{K}_j} \exp(c_i^\lambda/T))}{T} \right) \\ &= \exp \left(\frac{c_i - \sum_{k \in J_i} \lambda'_k}{T} \right) = \exp(c_i^{\lambda'}/T) \end{aligned} \quad (39)$$

□

Proof of Lemma 3. follows directly from Lemma 1 and Lemma 2. □

Proof of Proposition 6. The first part of the statement directly follows from the strong duality, Proposition 5 and Lemma 2. The second part follows from Lemma 7 that implies that after processing the clique \bar{K}_j it holds

$$\begin{aligned} \frac{\partial D^T}{\partial \lambda_j} &= 1 + \frac{\partial(T \sum_{i=1}^{n+m} \exp(c_i^\lambda/T))}{\partial \lambda_j} \\ &= 1 + T \sum_{i=1}^{n+m} \frac{\partial(\exp(c_i^\lambda/T))}{\partial \lambda_j} = 1 - \sum_{i \in \bar{K}_j} \exp(c_i^\lambda/T) \\ &\stackrel{\text{Lemma 2}}{=} 1 - \sum_{i \in \bar{K}_j} x_i \stackrel{\text{Algorithm 2}}{=} 0 \end{aligned} \quad (40)$$

□

Proof of Lemma 4. Initialization: $\hat{\mathbf{x}}$ is feasible by construction in Line 2. Exactly two coordinates in each

inequality $j \in J_i$ containing x_i are changing at each iteration of the loop over $i \in [n]$ in Lines 3 to 7: The value of \hat{x}_i is increased (Line 5) and the value of the respective slack \hat{x}_{n+j} is decreased by the same amount. So the sum of coordinates of $\hat{\mathbf{x}}$ in each clique constraint remains unchanged and equal to one. □

Proof of Lemma 5. As $\sum_{j \in \bar{K}_j} x_i = 1$ for all $j \in J_i$, it holds $M \geq x_i$ in Line 5. In turn it implies $\hat{x}_i = x_i$. □

Proof of Lemma 6. The mapping \mathcal{P} is continuous as a superposition of continuous mappings defined by Algorithm 5.

To prove the implication denote $\hat{\mathbf{x}} := \mathcal{P}(\mathbf{x})$ and note that $x_i \geq \hat{x}_i$ for any $i \in [n]$ by construction. The latter inequality holds as equality and, therefore, trivially satisfies the implication, unless there exist a constraint $j \in [m]$ such that $\hat{x}_{n+j} = 0$. Consider now

$$\begin{aligned} \epsilon &\geq \underbrace{\sum_{i' \in \bar{K}_j} x_{i'}}_{\leq 1+\epsilon} - \underbrace{\sum_{i' \in \bar{K}_j} \hat{x}_{i'}}_{=1} = \sum_{i' \in \bar{K}_j} \underbrace{(x_{i'} - \hat{x}_{i'})}_{\geq 0} + \underbrace{x_{n+j}}_{\geq 0} - \underbrace{\hat{x}_{n+j}}_{=0} \\ &\geq \sum_{i' \in \bar{K}_j} |x_{i'} - \hat{x}_{i'}| \stackrel{i \in \bar{K}_j}{\geq} |x_i - \hat{x}_i|. \end{aligned} \quad (41)$$

□

Proof of Lemma 7. Consider

$$\begin{aligned} \max_{\mathbf{x} \in [0,1]^{n+m}} \langle \mathbf{c}, \mathbf{x} \rangle - T \sum_{i=1}^{n+m} (x_i \log x_i - x_i) \\ = \sum_{i=1}^{n+m} \max_{x_i \in [0,1]} c_i x_i - T x_i \log x_i + T x_i. \end{aligned} \quad (42)$$

The function $f(x) := cx - Tx \log x + Tx$ of a scalar x dependent on scalars $c \leq 0$ and $T \geq 0$ is concave and therefore its optimum is defined by the following condition

$$0 = \nabla f(x) = c - T(\log x + x/x - 1) = c - T \log x. \quad (43)$$

It implies

$$\log x = c/T; \quad x = \exp(c/T). \quad (44)$$

Since $c \leq 0$, it holds $0 \leq x \leq 1$, i.e. it satisfies the box constraints constraints on x_i in (42).

The value of $f(x)$ in its maximum is computed as

$$\begin{aligned} \max_{x \in [0,1]} f(x) &= c \cdot \exp(c/T) - T \cdot \exp(c/T)(c/T) + T \exp(c/T) \\ &= T \cdot \exp(c/T). \end{aligned} \quad (45)$$

Putting all together leads to (24). □